

# Sorafenib promotes graft-versus-leukemia activity in mice and humans through IL-15 production in FLT3-ITD-mutant leukemia cells

Individuals with acute myeloid leukemia (AML) harboring an internal tandem duplication (ITD) in the gene encoding Fms-related tyrosine kinase 3 (FLT3) who relapse after allogeneic hematopoietic cell transplantation (allo-HCT) have a 1-year survival rate below 20%. We observed that sorafenib, a multitargeted tyrosine kinase inhibitor, increased IL-15 production by FLT3-ITD<sup>+</sup> leukemia cells. This synergized with the allogeneic CD8<sup>+</sup> T cell response, leading to long-term survival in six mouse models of FLT3-ITD<sup>+</sup> AML. Sorafenib-related IL-15 production caused an increase in CD8<sup>+</sup>CD107a<sup>+</sup>IFN- $\gamma$ <sup>+</sup> T cells with features of longevity (high levels of Bcl-2 and reduced PD-1 levels), which eradicated leukemia in secondary recipients. Mechanistically, sorafenib reduced expression of the transcription factor ATF4, thereby blocking negative regulation of interferon regulatory factor 7 (IRF7) activation, which enhanced IL-15 transcription. Both IRF7 knockdown and ATF4 overexpression in leukemia cells antagonized sorafenib-induced IL-15 production *in vitro*. Human FLT3-ITD<sup>+</sup> AML cells obtained from sorafenib responders following sorafenib therapy showed increased levels of IL-15, phosphorylated IRF7, and a transcriptionally active IRF7 chromatin state. The mitochondrial spare respiratory capacity and glycolytic capacity of CD8<sup>+</sup> T cells increased upon sorafenib treatment in sorafenib responders but not in nonresponders. Our findings indicate that the synergism of T cells and sorafenib is mediated via reduced ATF4 expression, causing activation of the IRF7–IL-15 axis in leukemia cells and thereby leading to metabolic reprogramming of leukemia-reactive T cells in humans. Therefore, sorafenib treatment has the potential to contribute to an immune-mediated cure of FLT3-ITD-mutant AML relapse, an otherwise fatal complication after allo-HCT.

ITDs in the gene encoding the FLT3 receptor tyrosine kinase are found in 20–25% of AML cases and provide a stimulus for persistent leukemia cell proliferation. Because of the unfavorable prognosis of FLT3-ITD<sup>+</sup> AML, most patients undergo allo-HCT<sup>1,2</sup>. FLT3-ITD<sup>+</sup> AML relapse after allo-HCT is not curable in the majority of patients. Sorafenib is a multitargeted tyrosine kinase inhibitor that can reduce the proliferation and survival of FLT3-ITD<sup>+</sup> AML cells *in vitro*. Although sorafenib treatment did not improve the overall survival (OS) of patients with AML when combined with standard chemotherapy<sup>3,4</sup>, it caused durable remission in some patients with FLT3-ITD<sup>+</sup> AML after allo-HCT<sup>5–7</sup>, thereby prompting trials of sorafenib maintenance therapy<sup>8–11</sup>. However, the mechanism by which sorafenib combined with allogeneic immunity may induce long-term control of FLT3-ITD<sup>+</sup> AML remains unknown.

## RESULTS

### Sorafenib induces IL-15 production by FLT3-ITD<sup>+</sup> AML cells

To understand whether a functional synergism between allogeneic immune responses and sorafenib occurs, we used a mouse leukemia model<sup>12</sup> in which one allele of mixed-lineage leukemia (*Mll*) has a partial tandem duplication (*Mll*<sup>PTD/+</sup>) and one *Flt3* allele has the ITD mutation (*Flt3*<sup>ITD/+</sup>) (Fig. 1a). Leukemia cells from these mice were infused into recipient mice after irradiation and allo-HCT and 2 d after allo-HCT donor-derived T cells were infused, in a procedure

analogous to donor lymphocyte infusions (DLI) in patients. We observed long-term control of leukemia only in mice receiving both sorafenib and T cells. Sorafenib was not protective when administered alone (Fig. 1a). A comparable pattern of leukemia control was observed using a mouse model of lymphoblastic leukemia (in which mice are injected with the mouse Ba/F3-ITD cell line) with respect to survival (Fig. 1b) and expansion of luciferase reporter (LUC)<sup>+</sup>GFP<sup>+</sup> leukemia cells (Fig. 1c–e and Supplementary Fig. 1a). Microarray-based analysis of Ba/F3-ITD cells revealed that IL-15 (*Il15*) mRNA was upregulated upon sorafenib exposure *in vitro* (Fig. 1f,g), which was confirmed through qPCR and flow cytometry (Fig. 1h,i). IL-15 production was dependent on sorafenib sensitivity, as Ba/F3 cells expressing the sorafenib-resistant FLT3-ITD-F691L mutant showed no increase in IL-15 expression following sorafenib treatment (Fig. 1i).

IL-15 levels were higher in serum from mice that were treated with T cells and sorafenib than in vehicle-treated mice (Fig. 1j). This sorafenib-induced increase in serum IL-15 subsided with reduced numbers of leukemia cells at a later time point during treatment (Fig. 1j). IL-15 serum levels increased upon FLT3-ITD inhibition in additional mouse models of myeloid leukemia (including models in which mice were injected with bone marrow (BM) cells transfected with FLT3-ITD or the mouse myeloid WEHI-3B<sup>FLT3-ITD</sup> cell line, and the genetic model driven by the *Mll*<sup>PTD/+</sup> and *Flt3*<sup>ITD/+</sup> mutations<sup>13</sup>)

A full list of authors and affiliations appears at the end of the paper.

Received 10 July 2016; accepted 5 January 2018; published online 12 February 2018; corrected after print 6 March 2018; doi:10.1038/nm.4484

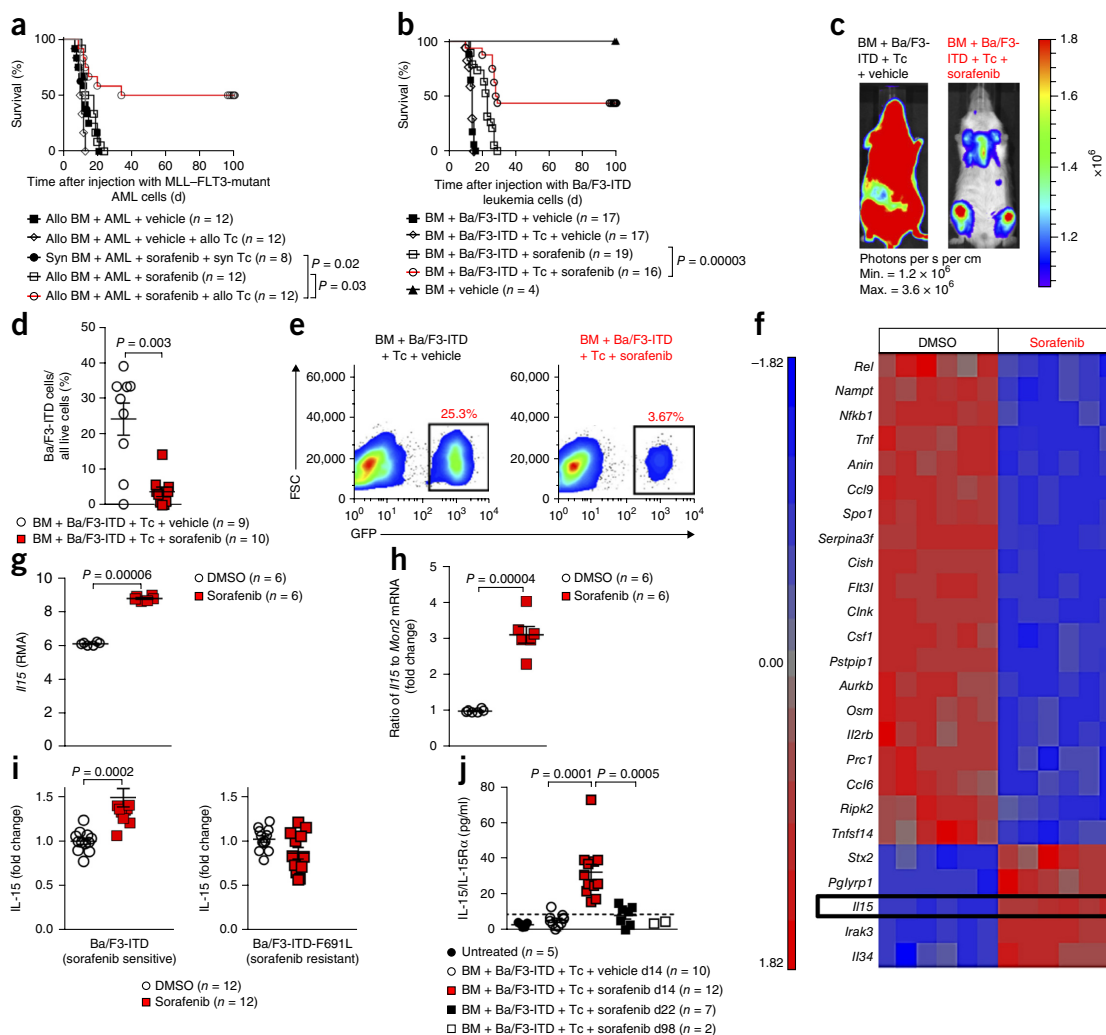


**Figure 1** Sorafenib synergizes with allogeneic T cells and improves survival in mouse models of FLT3-ITD-driven AML through increasing IL-15 production. **(a)** Percentage survival of recipient mice (C57BL/6 background) transplanted with leukemia cells from the *Mll<sup>ITD/+</sup>; Fli3<sup>ITD/+</sup>* AML model (C57BL/6 background) and BALB/c BM (allo BM) or C57BL/6 BM (syn BM) with or without additional BALB/c T cells (allo Tc) or C57BL/6 T cells (syn Tc) and treated with either vehicle or sorafenib. The experiment was performed twice, and the results were pooled; *n* values represent biologically independent (unrelated) mice. *P* values were calculated using the two-sided Mantel–Cox test. **(b)** Percentage survival of BALB/c recipients transplanted with C57BL/6 BM and Ba/F3-ITD leukemia cells with or without additional C57BL/6 T cells and treated with vehicle or sorafenib as in **a**. The experiment was performed three times, and the results were pooled; *n* values represent biologically independent mice. *P* values were calculated using the two-sided Mantel–Cox test. **(c)** Bioluminescence imaging (BLI) on day 10 after transplantation with LUC<sup>+</sup> Ba/F3-ITD leukemia cells showing the expansion of Ba/F3-ITD cells in BALB/c recipients also transplanted with C57BL/6 BM and T cells and treated with vehicle or sorafenib. Images are of a representative mouse from each of the two groups. **(d,e)** BALB/c recipient mice were transplanted with C57BL/6 BM and Ba/F3-ITD leukemia cells with additional C57BL/6 T cells and were treated with vehicle or sorafenib. **(d)** Percentage of Ba/F3-ITD cells in the spleen 14 d after transplantation. The experiment was performed three times, and the results (mean ± s.e.m.) were pooled; *n* values represent biologically independent mice. *P* values were calculated using the two-sided Student's unpaired *t*-test. **(e)** Representative flow cytometry plots showing the percentage of GFP<sup>+</sup> Ba/F3-ITD cells in the spleens of mice from each group. The data are representative of one of three independent experiments. FSC, forward scatter. **(f,g)** Ba/F3-ITD leukemia cells were treated with sorafenib (10 nM) or DMSO alone for 24 h. **(f)** Microarray-based analysis of gene expression. Tile display shows the 25 most significantly differentially regulated genes as determined from robust multichip average (RMA) signal values. The scale represents the level of gene expression with red being highest and blue being lowest. **(g)** RMA values of *Il15* in Ba/F3-ITD cells; *n* values represent biologically independent samples. *P* values were calculated using the two-sided Student's unpaired *t*-test. **(h)** Quantification of *Il15* mRNA expression through qPCR in Ba/F3-ITD leukemia cells treated with 10 nM sorafenib or DMSO relative to *Mon2* mRNA expression. The experiment was performed three times, and the results (mean ± s.e.m.) were pooled; *n* values represent biologically independent samples. *P* values were calculated using the two-sided Student's unpaired *t*-test. **(i)** Quantification of intracellular IL-15 (fold change in the mean fluorescence intensity (MFI) of IL-15 with respect to the mean MFI of IL-15 in DMSO-treated controls). Ba/F3-ITD cells (sorafenib sensitive) and Ba/F3-ITD-F691L cells (harboring a mutation in *FLT3* conferring sorafenib resistance) were studied. The experiment was performed three times, and the results (mean ± s.e.m.) were pooled; *n* values represent biologically independent samples, and each data point represents a measurement from a biologically independent sample. *P* values were calculated using the two-sided Student's unpaired *t*-test. **(j)** Quantification of serum IL-15 and IL-15Rα from naive BALB/c mice or BALB/c recipients transplanted with C57BL/6 BM and Ba/F3-ITD leukemia cells with additional C57BL/6 T cells and treated with vehicle or sorafenib on day 14, day 22, or day 98 following intravenous (i.v.) injection of Ba/F3-ITD cells. The dashed line represents the detection limit (4 pg/ml) for the mouse IL-15 and IL-15Rα ELISA. The experiment was performed three times (except one time for the day 98 group), and the results (mean ± s.e.m.) were pooled; *n* values represent biologically independent samples, and each data point represents a measurement from a biologically independent sample derived from an individual mouse. *P* values were calculated using a two-sided Mann–Whitney *U* test.

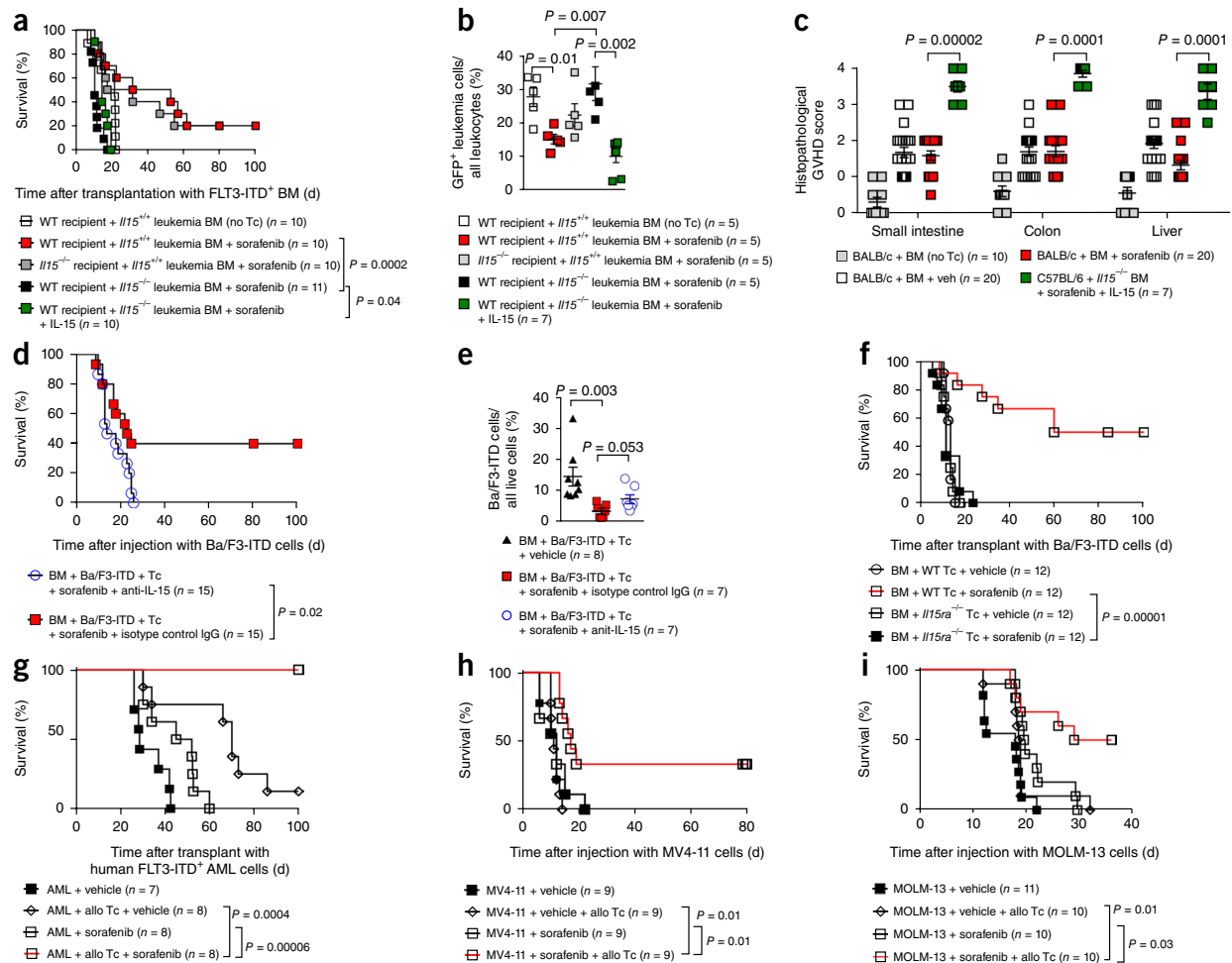


**Figure 2** Sorafenib-induced IL-15 production derives from leukemia cells *in vivo* and synergizes with T cells in humanized mouse models.

(a) The survival rate of C57BL/6 mice transplanted with wild-type (WT) BALB/c BM together with GFP<sup>+</sup> FLT3-ITD<sup>+</sup> C57BL/6 BM to induce leukemia. Two days following transplant, BALB/c T cells were injected to induce the allogeneic immune effect. The FLT3-ITD<sup>+</sup> BM was derived from either WT C57BL/6 mice or *Il15*<sup>-/-</sup> C57BL/6 mice to generate IL-15-deficient leukemia cells. There were four experimental conditions: WT C57BL/6 mice were transplanted with BALB/c BM, FLT3-ITD<sup>+</sup>/*Il15*<sup>+/+</sup> C57BL/6 BM, and BALB/c T cells and treated with sorafenib (red squares); *Il15*<sup>-/-</sup> C57BL/6 mice were transplanted with BALB/c BM, FLT3-ITD<sup>+</sup>/*Il15*<sup>+/+</sup> C57BL/6 BM, and BALB/c T cells and treated with sorafenib (gray squares); WT C57BL/6 mice were transplanted with BALB/c BM, FLT3-ITD<sup>+</sup>/*Il15*<sup>-/-</sup> C57BL/6 BM, and BALB/c T cells and treated with sorafenib (black squares); and WT C57BL/6 recipients were transplanted with BALB/c BM, FLT3-ITD<sup>+</sup>/*Il15*<sup>-/-</sup> C57BL/6 BM, and BALB/c T cells and treated with sorafenib and IL-15 (green squares). The experiment was performed twice, and the results were pooled; *n* values represent biologically independent mice. *P* values were calculated using the two-sided Mantel–Cox test. (b) The percentage of GFP<sup>+</sup> FLT3-ITD<sup>+</sup> BM cells, derived as described in a, among all leukocytes in the blood of mice on day 14 from the groups in a. The experiment was performed twice and the results (mean ± s.e.m.) were pooled; *n* values represent biologically independent mice. The *P* values were calculated using the two-sided Mann–Whitney *U* test. (c) Histopathological scores from different GVHD target organs isolated on day 10 following allo-HCT from BALB/c recipient mice transplanted with FLT3-ITD<sup>+</sup> BM cells and T cells and treated with vehicle or sorafenib or from C57BL/6 recipients transplanted with FLT3-ITD<sup>+</sup> BM cells and T cells and treated with sorafenib and IL-15. The experiment was performed twice, and the results (mean ± s.e.m.) were pooled; *n* values represent biologically independent mice. The *P* values were calculated using the two-sided Mann–Whitney *U* test. (d) Percentage survival of BALB/c mice injected with C57BL/6 BM and Ba/F3-ITD leukemia cells and additional C57BL/6 T cells and treated with sorafenib together with nonspecific IgG or anti-IL-15 antibody. The experiment was performed three times, and the results were pooled; *n* values represent biologically independent mice. *P* values were calculated using the two-sided Mantel–Cox test. (e) Percentage of GFP<sup>+</sup> Ba/F3-ITD leukemia cells among all live cells in spleens from the mice described in d and an additional vehicle-treated group on day 14 following transplantation. The experiment was performed two times, and the results (mean ± s.e.m.) were pooled; *n* values represent biologically independent mice. *P* values were calculated using the two-sided Mann–Whitney *U* test. (f) The survival rate of BALB/c recipients injected with Ba/F3-ITD leukemia cells. Mice were transplanted with C57BL/6 WT BM (day 0) and with additional C57BL/6 WT T cells or *Il15ra*<sup>-/-</sup> T cells (day 2). The experiment was performed twice with similar results; *n* values represent biologically independent mice. *P* values were calculated using the two-sided Mantel–Cox test. (g) Percentage survival of NSG mice injected with primary human FLT3-ITD<sup>+</sup> AML cells derived from an HLA-A2<sup>+</sup> patient with or without additional allogeneic human CD8<sup>+</sup> T cells that had been stimulated and expanded in the presence of autologous dendritic cells (DCs) expressing allogeneic HLA-A2 upon RNA transfection *in vitro*. Mice were treated with vehicle or sorafenib as indicated. The experiment was performed twice with similar results; *n* values represent biologically independent mice. *P* values were calculated using the two-sided Mantel–Cox test. (h) Percentage survival of *Rag2*<sup>-/-</sup>/*Il2ra*<sup>-/-</sup> mice following transplantation with human MV4-11 FLT3-ITD<sup>+</sup> leukemia cells with or without additional C57BL/6 T cells and treatment with vehicle or sorafenib. The experiment was performed three times, and the results were pooled; *n* values represent biologically independent mice. *P* values were calculated using the two-sided Mantel–Cox test. (i) Percentage survival of *Rag2*<sup>-/-</sup>/*Il2ra*<sup>-/-</sup> mice following transplantation with human FLT3-ITD<sup>+</sup> MOLM-13 cells with or without additional C57BL/6 T cells and treatment with vehicle or sorafenib. The experiment was performed once; *n* values represent biologically independent mice. *P* values were calculated using the two-sided Mantel–Cox test.

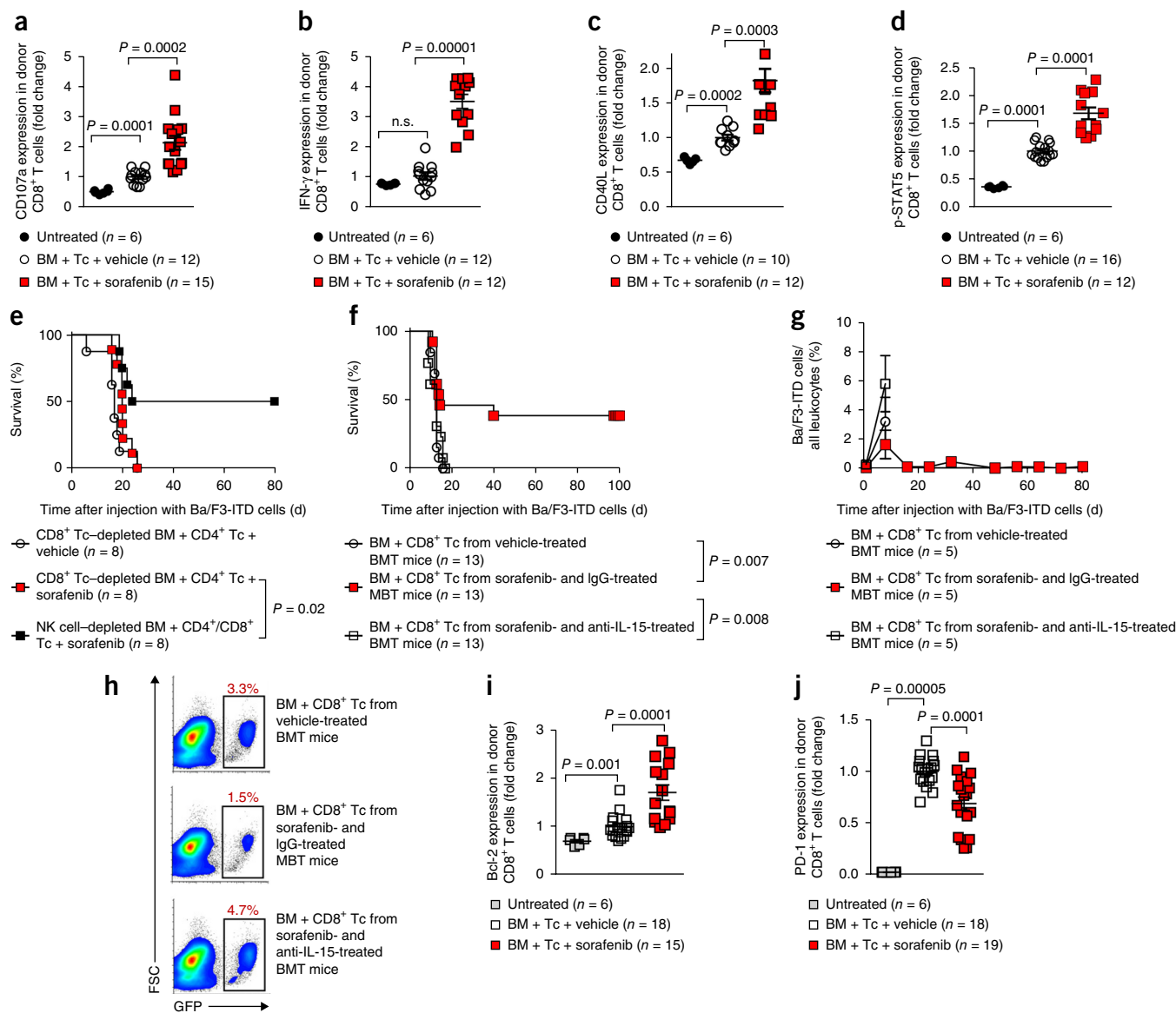


**Figure 3** Sorafenib promotes cytotoxicity and longevity of donor CD8<sup>+</sup> T cells via IL-15. **(a–d)** Flow cytometry analysis of spleens from BALB/c mice transplanted with C57BL/6 BM, Ba/F3-ITD leukemia cells (day 0), and C57BL/6 T cells (day 2) as described in **Figure 1b**. The time point of analysis is day 12 following Ba/F3-ITD i.v. injection. Plots show the fold change in MFI (with respect to the mean MFI of the vehicle-treated group) for CD107a **(a)**, IFN- $\gamma$  **(b)**, CD40L **(c)**, and p-STAT5 **(d)** in all live H-2kb<sup>+</sup>CD8<sup>+</sup> T cells from BM-transplanted mice treated with vehicle or sorafenib as indicated or from untreated naive C57BL/6 mice. For **a–d**, each data point represents an individual sample of one biologically independent mouse. The experiments were repeated three times, and the results (mean  $\pm$  s.e.m.) were pooled;  $n$  values represent biologically independent mice.  $P$  values were calculated using the two-sided Student's unpaired  $t$ -test. **(e)** Percentage survival of BALB/c mice injected with Ba/F3-ITD leukemia cells, CD8<sup>+</sup> T cell-depleted C57BL/6 BM, and CD4<sup>+</sup> T cells and treated with either sorafenib or vehicle or injected with Ba/F3-ITD leukemia cells, NK (NK1.1<sup>+</sup>) cell-depleted C57BL/6 BM, and T cells and treated with vehicle or sorafenib. The experiment was repeated twice, and the results were pooled;  $n$  values represent biologically independent mice.  $P$  values were calculated using the two-sided Mantel–Cox test. **(f)** Percentage survival of BALB/c mice (secondary recipients) that were transplanted with C57BL/6 BM ( $5 \times 10^6$ ), Ba/F3-ITD leukemia cells (day 0), and H-2kb<sup>+</sup>CD3<sup>+</sup>CD8<sup>+</sup> T cells (day 2) from the spleens of BALB/c mice (primary recipients (BMT mice); 12 d after BM transplant) that had been injected with C57BL/6 BM ( $5 \times 10^6$ ), allogenic CD4<sup>+</sup> and CD8<sup>+</sup> T cells ( $2 \times 10^5$ ), and Ba/F3-ITD leukemia cells and treated with vehicle or sorafenib together with isotype control IgG or anti-IL-15 antibody. The experiment was performed three times, and the results were pooled;  $n$  values represent biologically independent mice.  $P$  values were calculated using the two-sided Mantel–Cox test. **(g)** Flow cytometry measuring GFP<sup>+</sup> Ba/F3-ITD cells (as a percentage of all leukocytes) in blood from the different groups in **f** at different time points following transplantation. The experiment was performed twice, and the results (mean  $\pm$  s.e.m.) were pooled;  $n$  values represent biologically independent mice. **(h)** A representative flow cytometry plot from one mouse per group showing the percentage of GFP<sup>+</sup> Ba/F3-ITD leukemia cells (among all leukocytes) in spleens on day 8 following transplantation of Ba/F3-ITD cells from different groups as in **f**. **(i, j)** Expression of Bcl-2 **(i)** and PD-1 **(j)** (quantified as fold change in the MFI with respect to the mean MFI for the vehicle-treated group) in all H-2kb<sup>+</sup>CD8<sup>+</sup> T cells from BMT mice transplanted with Ba/F3-ITD cells and treated with vehicle or sorafenib as indicated or from untreated naive C57BL/6 mice. Each data point represents an individual sample of one biologically independent animal. The experiment was performed three times, and the results (mean  $\pm$  s.e.m.) were pooled;  $n$  values represent biologically independent mice.  $P$  values were calculated using a two-sided Mann–Whitney  $U$  test **(i)** or a two-sided Student's unpaired  $t$ -test **(j)**.

(Supplementary Fig. 1b–d). Sorafenib had no effect on T cell activation *in vitro* (Supplementary Fig. 1e–h). Leukemia cells expressed IL-15 receptor subunit  $\alpha$  (IL-15R $\alpha$ ; Supplementary Fig. 1i,j), which is essential for IL-15 transpresentation<sup>14</sup>.

Genetic deficiency for IL-15 in FLT3-ITD<sup>+</sup> leukemia cells abrogated the beneficial effects of sorafenib, whereas IL-15 deficiency of the recipient mouse did not (Fig. 2a,b). Lack of IL-15 in leukemia cells could be rescued by exogenous IL-15 (Fig. 2b); however, this resulted

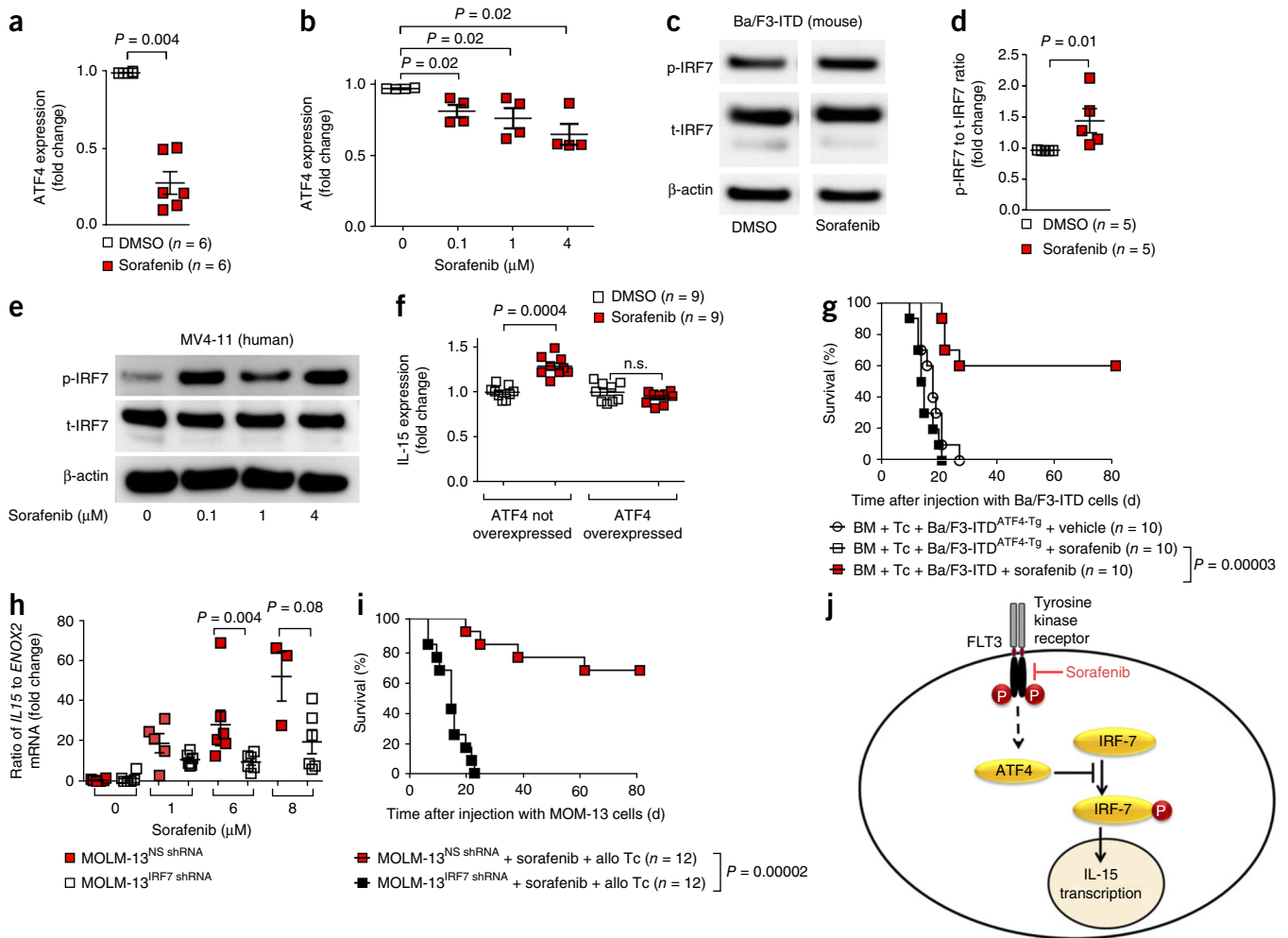


**Figure 4** Sorafenib induces phosphorylation of IRF7 via reducing levels of its inhibitor ATF4. (a,b) Quantification of ATF4 expression (by western blot) normalized to that of  $\beta$ -actin (quantified as the fold change with respect to DMSO-treated controls) in mouse Ba/F3-ITD (a) or human FLT3-ITD<sup>+</sup> MV4-11 (b) leukemia cells exposed to sorafenib as indicated. The experiments were performed three times, and the results (mean  $\pm$  s.e.m.) were pooled;  $n$  values represent biologically independent samples.  $P$  values were calculated using the two-sided Mann–Whitney  $U$  test. (c) Western blots showing the levels of p-IRF7, t-IRF7, and loading control ( $\beta$ -actin) in Ba/F3-ITD leukemia cells exposed to sorafenib. All uncropped western blots are shown in Supplementary Figures 15–21. (d) Quantification of p-IRF7 to t-IRF7 ratio normalized to the level of  $\beta$ -actin (quantified as fold change with respect to DMSO-treated controls) in Ba/F3-ITD cells treated as indicated. The experiment was performed four times, and the results (mean  $\pm$  s.e.m.) were pooled;  $n$  values represent biologically independent samples, and each data point represents an individual sample of one independent cell culture experiment.  $P$  values were calculated using the two-sided Mann–Whitney  $U$  test. (e) Representative western blots showing the levels of p-IRF7, t-IRF7, and loading control ( $\beta$ -actin) in MV4-11 cells treated with the indicated sorafenib concentrations for 24 h. (f) Fold change of intracellular IL-15 (MFI) in Ba/F3-ITD cells or Ba/F3-ITD cells transfected with a lentiviral vector overexpressing mouse ATF4 and treated with sorafenib (0.1  $\mu$ M) as indicated for 24 h. Fold change is relative to DMSO treatment, which is set as ‘1’. The experiment was performed three times, and results (mean  $\pm$  s.e.m.) were pooled;  $n$  values represent biologically independent samples, and each data point represents an individual sample of one independent cell culture experiment.  $P$  values were calculated using the two-sided Mann–Whitney  $U$  test. (g) Percentage survival of BALB/c mice transplanted with C57BL/6 BM and ATF4-overexpressing Ba/F3-ITD cells or Ba/F3-ITD cells with endogenous ATF4 expression (Ba/F3-ITD<sup>ATF4-Tg</sup> and Ba/F3-ITD, respectively;  $n = 500$  cells) with additional C57BL/6 T cells ( $2 \times 10^5$ , administered on day 2) and treated with vehicle or sorafenib. The experiment was performed twice, and the results were pooled;  $n$  values represent biologically independent mice.  $P$  values were calculated using the two-sided Mantel–Cox test. (h) Quantification of *IL15* mRNA through qPCR in human MOLM-13 (FLT3-ITD<sup>+</sup> AML) cells expressing a nonsilencing vector (MOLM-13<sup>NS shRNA</sup>) or an IRF7-knockdown vector (MOLM-13<sup>IRF7 shRNA</sup>). MOLM-13 cells were exposed to the indicated concentrations of sorafenib. The experiment was performed twice, and the results (mean  $\pm$  s.e.m.) were pooled;  $n$  values represent biologically independent samples.  $P$  values were calculated using the two-sided Mann–Whitney  $U$  test. (i) Percentage survival of *Rag2*<sup>-/-</sup> *Il2ra*<sup>-/-</sup> mice transplanted with MOLM-13<sup>NS shRNA</sup> or MOLM-13<sup>IRF7 shRNA</sup> cells as indicated. The experiment was performed twice, and the results were pooled;  $n$  values represent biologically independent mice. The  $P$  value was calculated using a two-sided Mantel–Cox test. (j) Proposed mechanism through which sorafenib leads to increased IL-15 transcription. Sorafenib inhibits FLT3 receptor tyrosine kinase signaling, which normally leads to ATF4 production. Reduced ATF4 levels result in less inhibition of IRF7 phosphorylation and activation. Active p-IRF7 can translocate to the nucleus, where it activates IL-15 transcription.

in increased lethality (Fig. 2a) due to more severe graft-versus-host disease (GVHD), which was not observed in sorafenib-treated mice (Fig. 2c). These data indicate that the level of IL-15 production by leukemia cells following sorafenib exposure was below the threshold required to drive a GVHD response.

Antibody-based IL-15 depletion or transfer of *Il15ra*-deficient T cells to recipient mice caused loss of leukemia control despite sorafenib treatment (Fig. 2d–f). The sorafenib–T cell combination improved survival in recipient mice transfused with leukemia cells from three humanized models in which mice were injected with primary human FLT3-ITD<sup>+</sup> AML cells or cells from the MV4-11 or MOLM-13 human cell line (both of which are FLT3-ITD<sup>+</sup> AML cell lines) (Fig. 2g–i).

### T cells from sorafenib-treated mice exhibit an activated phenotype and reject leukemia cells in secondary recipients

Expression of the antitumor cytotoxicity marker<sup>15</sup> CD107a, interferon (IFN)- $\gamma$ , and CD40 ligand (CD40L) was higher in donor CD8<sup>+</sup> T cells in allo-HCT recipients that had been treated with sorafenib than in those that were treated with vehicle (Fig. 3a–c and Supplementary Fig. 2a,b). Treatment with IL-15 increased the frequency of CD8<sup>+</sup>CD107a<sup>+</sup> T cells *in vitro* as compared to vehicle treatment (Supplementary Fig. 2c,d). IL-15R activation leads to signal transducer and activator of transcription 5 (STAT5) phosphorylation<sup>16</sup>, and higher levels of phosphorylated STAT5 (p-STAT5) were found in CD8<sup>+</sup> T cells derived from sorafenib-treated mice (Fig. 3d). Depletion of CD8<sup>+</sup> T cells, but not natural killer (NK) cells (Supplementary Fig. 2e), in grafts caused loss of the protective effect of sorafenib (Fig. 3e), indicating that CD8<sup>+</sup> T cells mediate the sorafenib-induced antitumor effect.

To understand whether recall immunity developed under sorafenib treatment, we next isolated CD8<sup>+</sup>H-2Kb<sup>+</sup> T cells from mice transfused with Ba/F3-ITD leukemia cells that had been treated with T cells and either vehicle or sorafenib (Supplementary Fig. 2f). We transplanted these cells into secondary recipients of Ba/F3-ITD leukemia cells, finding that CD8<sup>+</sup>H-2Kb<sup>+</sup> T cells isolated from allo-HCT recipients that had been treated with sorafenib, but not those from mice treated with vehicle or with anti-IL-15 antibody in addition to sorafenib, caused long-term control in secondary recipients (Fig. 3f–h). Donor T cells from sorafenib-treated primary recipients exhibited features of longevity<sup>17,18</sup>, including high expression of B cell lymphoma 2 (Bcl-2) and reduced programmed cell death protein 1 (PD-1) expression (Fig. 3i,j).

The target specificity of the recall immune response was reflected by the fact that T cells isolated from sorafenib-treated primary recipients bearing leukemia cells of the Ba/F3-ITD line did not control leukemia resulting from WEHI-3B cells from third-party donors in secondary recipients (Supplementary Fig. 2g–i). *In vitro* IL-15 production was not seen in FLT3-ITD<sup>-</sup> leukemia cell lines upon sorafenib exposure (Supplementary Fig. 3a,b), and FLT3-ITD<sup>-</sup> WEHI-3B cells could not induce recall immunity (Supplementary Fig. 3c,d).

### Sorafenib induces IL-15 production via ATF4 inhibition

IRF7 is an essential upstream activator of IL-15 transcription<sup>19,20</sup>. Activating transcription factor-4 (ATF4) blocks IRF7 phosphorylation and activation<sup>21</sup>, thereby preventing IL-15 transcription. We observed reduced levels of *Atf4* mRNA and ATF4 protein in mouse and human cells with FLT3-ITD-driven leukemia, but not in sorafenib-resistant FLT3-ITD<sup>+</sup> or FLT3-ITD<sup>-</sup> leukemia cells, upon sorafenib exposure (Fig. 4a,b and Supplementary Fig. 4a–f). In accordance with the hypothesis of decreased negative regulation by ATF4 in FLT3-ITD<sup>+</sup>

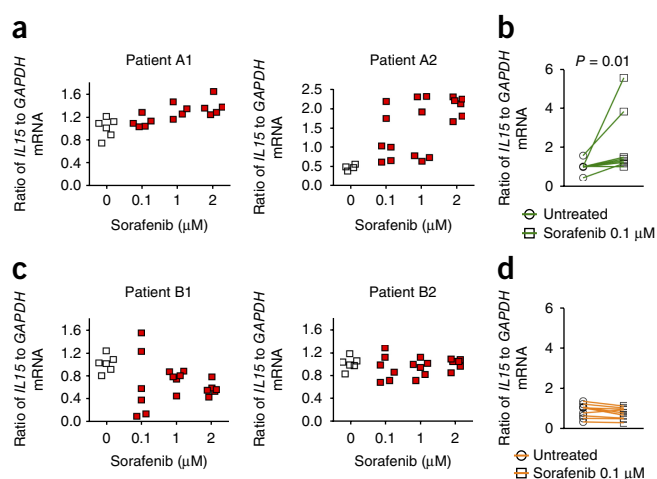


**Figure 5** Treatment with sorafenib induces IL-15 in human primary FLT3-ITD<sup>+</sup> leukemia cells. (a) Representative *IL15* mRNA expression determined through qPCR of primary human FLT3-ITD<sup>+</sup> AML cells. Six technical replicates from two independent patients per group are shown. As these results display only representative data from technical replicates, no statistical analysis was performed. (b) Cumulative *IL15* mRNA levels determined through qPCR of primary human FLT3-ITD<sup>+</sup> AML cells (from  $n = 8$  biologically independent patients). The  $P$  value was calculated using the two-sided Wilcoxon matched-pairs signed-rank test. (c) Representative ratio of *IL15* mRNA expression determined through qPCR of primary human FLT3-ITD<sup>-</sup> AML cells. Six technical replicates from two independent patients per group are shown. As these results display only representative data from technical replicates, no statistical analysis was performed. (d) Cumulative *IL15* mRNA levels determined through qPCR of primary human FLT3-ITD<sup>-</sup> AML cells ( $n = 10$  biologically independent patients). For a–d, each data point indicates the ratio of *IL15* to *GAPDH* mRNA in the AML cells that were untreated or exposed to sorafenib as indicated.

leukemia cells, the amount of active IRF7 (assessed by p-IRF7 and total IRF7 (t-IRF7, meaning unphosphorylated IRF7)) increased upon sorafenib treatment in mouse and human FLT3-ITD<sup>+</sup> leukemia cells (Fig. 4c–e and Supplementary Fig. 4g), but not in sorafenib-resistant FLT3-ITD<sup>+</sup> leukemia cells (Supplementary Fig. 4h). The increased IL-15 production (Fig. 4f), IRF7 activation (Supplementary Fig. 4i,j), extended survival (Fig. 4g), and reduced counts of leukemia cells in peripheral blood (Supplementary Fig. 4k) resulting from sorafenib treatment were abrogated by ATF4 overexpression in leukemia cells (Supplementary Fig. 4l). IRF7 knockdown in leukemia cells (Supplementary Fig. 4m) caused reduced levels of IL-15 production by human FLT3-ITD<sup>+</sup> AML cells *in vitro* and loss of extended survival upon sorafenib treatment *in vivo* (Fig. 4h,i).

Kinome analysis and subsequent kinase inhibition of human FLT3-ITD<sup>+</sup> AML cells revealed the selective impact of sorafenib on IL-15 production (Supplementary Figs. 5 and 6). Analysis of the kinases binding sorafenib identified none other than FLT3 directly linked to IL-15 production (Supplementary Fig. 7). On the basis of these observations, we propose a mechanism through which sorafenib increases IL-15 production via inhibition of the negative regulatory function of ATF4 in FLT3-ITD<sup>+</sup> AML, resulting in IRF7 activation (Fig. 4j).

### T cells isolated from patients responding to sorafenib exhibit increased mitochondrial fitness

Like sorafenib, other FLT3 inhibitors increased IL-15 production (Supplementary Fig. 8a–q). In accordance with our findings in mouse

leukemia cells, we observed that *in vitro* sorafenib exposure increased *IL15* mRNA levels in primary human FLT3-ITD<sup>+</sup> AML cells, but not in FLT3-ITD<sup>-</sup> AML cells (Fig. 5a–d). Additionally, IL-15 serum levels, levels of IL-15 and p-IRF7 protein in BM, and *IL15* mRNA levels in leukemia cells increased in individuals with FLT3-ITD<sup>+</sup> AML upon sorafenib treatment (Fig. 6a–c and Supplementary Fig. 9a–c) and declined when leukemia burden was reduced (Supplementary Fig. 9d). We separately analyzed responders (hematologic complete remission was attained after treatment with DLI and sorafenib) and nonresponders (complete remission was not attained). The increase in IL-15 and p-IRF7 levels was not seen in nonresponders (Fig. 6a–c), and no increase was seen for other cytokines (Supplementary Fig. 9e–i). Increased IFN- $\gamma$  serum levels (Fig. 6d) and increased

frequency of IFN- $\gamma$ <sup>+</sup>CD8<sup>+</sup> T cells (Supplementary Fig. 9j,k) were found in DLI–sorafenib responders. Furthermore, the frequency of perforin<sup>+</sup>CD8<sup>+</sup> T cells was increased in DLI–sorafenib responders but not in nonresponders (Supplementary Fig. 9l,m).

Whole-genome sequencing of human primary FLT3-ITD<sup>+</sup> AML cells indicated a variable frequency of somatic mutations and copy number alterations regardless of membership in the responder or non-responder group (Supplementary Fig. 10a–c). Mutations conferring resistance to the FLT3 inhibitor (encoding FLT3-D839G and FLT3-D835Y<sup>22</sup>) were detected in several nonresponders but not in responders (Supplementary Fig. 10d). We annotated all mutations within a given distance of the transcription start sites of IRF family genes and found a reduction in the number of germline mutations affecting

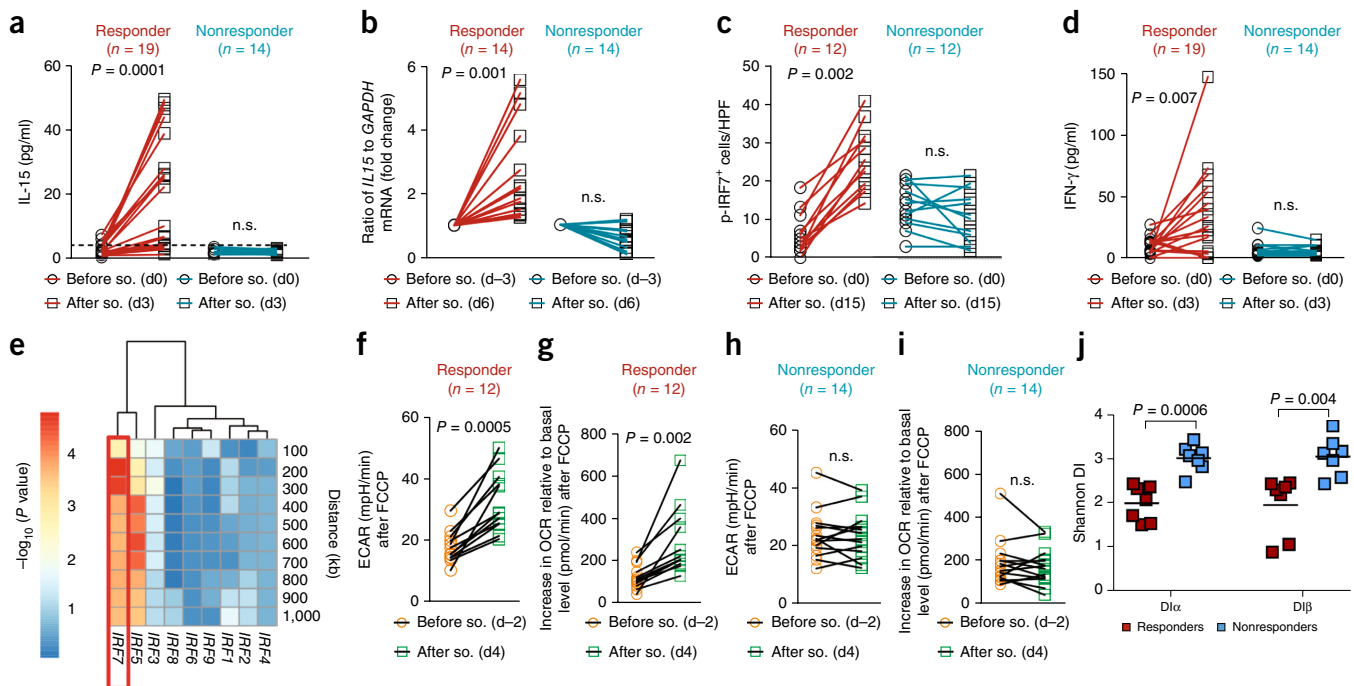


**Figure 6** Treatment with sorafenib increases the frequency of T cells that are actively glycolytic in patients with FLT3-ITD<sup>+</sup> AML who relapse after allo-HCT. (a) IL-15 levels in the serum of patients who relapsed with FLT3-ITD<sup>+</sup> AML after allo-HCT. Sorafenib–DLI responders and nonresponders are shown separately. Each data point represents the IL-15 level in the serum of a patient before sorafenib (so.) treatment (day 0) and after the start of sorafenib treatment (day 3; before the patients received DLI). The dashed line indicates the detection limit (4 pg/ml) of the IL-15 ELISA. *n* values represent biologically independent patients. The *P* value was determined using the two-sided Wilcoxon matched-pairs signed-rank test. (b) Quantification of *IL15* mRNA expression through qPCR of leukemia cells (>90% purity) derived from the peripheral blood of patients with FLT3-ITD<sup>+</sup> AML before (day –3) and after (day 6) the start of sorafenib treatment. Fold change is relative to the time point before sorafenib treatment, which is set as ‘1’. Each data point represents the ratio of *IL15* to *GAPDH* mRNA expression from an individual patient at the indicated time point. *n* values represent biologically independent patients. The *P* value was determined using the two-sided Wilcoxon matched-pairs signed-rank test. (c) Quantification of the number of p-IRF7<sup>+</sup> cells per high-power field (HPF) in BM biopsies from patients with FLT3-ITD<sup>+</sup> AML before (day 0) and after (day 15) the start of sorafenib treatment. Each data point represents the measurement of an individual patient at the indicated time point. *n* values represent biologically independent patients. The *P* value was determined using the two-sided Wilcoxon matched-pairs signed-rank test. (d) IFN- $\gamma$  levels in serum from patients who relapsed with FLT3-ITD<sup>+</sup> AML after allo-HCT. Each data point represents the IFN- $\gamma$  level in serum from a patient before (day 0) and after the start of sorafenib treatment (day 3; before the patients received DLI). *n* values represent biologically independent patients. The *P* value was determined using the two-sided Wilcoxon matched-pairs signed-rank test. (e) Heat map displaying the significance of having a smaller number of germline and somatic mutations in chromatin states marked as Tx (strong transcription) or TxW (weak transcription) around the transcription start sites of various IRF family genes for nonresponders (*n* = 4 biologically independent patients) versus responders (*n* = 4 biologically independent patients). IRF genes are hierarchically clustered by their Euclidean distance using the complete linkage algorithm. Significance of mutation frequencies was calculated from ANOVA with a *post hoc* Tukey’s test. *P* values for the comparison of the different IRFs for responders versus nonresponders were as follows: IRF7, *P* = 0.0005; IRF5, *P* = 0.001 (like IRF7, IRF5 activation induces IFN responses<sup>37</sup>); IRF1–IRF4 and IRF6–IRF9, not significant. (f–i) Metabolic profiling of CD8<sup>+</sup> T cells derived from the peripheral blood of patients with FLT3-ITD<sup>+</sup> AML before (day –2) and after (day 4) the start of sorafenib treatment, following FCCP exposure. Cells were profiled for ECAR in responders (f) and nonresponders (h) and for OCR relative to the basal level in responders (g) and nonresponders (i). Each data point represents the measurement of an individual patient at the indicated time point; *n* values represent biologically independent patients. *P* values were determined using the two-sided Wilcoxon matched-pairs signed-rank test. (j) Comparison of the median DI of the TCR $\alpha$  and TCR $\beta$  CDR3 amino acid sequences between responders and nonresponders. The analysis was performed on CD3<sup>+</sup> cells isolated from responders (*n* = 7 biologically independent patients) and nonresponders (*n* = 7 biologically independent patients) on day 30 after the start of sorafenib treatment. The *P* value was determined using the two-sided Mann–Whitney *U* test. No adjustments were made for multiple comparisons.

sites with strong (Tx) and weak (TxW) transcription around *IRF7* in the AML cells of DLI-sorafenib nonresponders as compared to DLI-sorafenib responders (Fig. 6e). The transcription start sites of IRF family genes were based on chromatin state data from monocytes. *IL15* mRNA expression was upregulated after sorafenib treatment only in responders (Supplementary Fig. 11a).

Mitochondrial spare respiratory capacity (SRC) and glycolytic capacity (GC) have been linked to prolonged T cell survival and enhanced ability to respond to antigen challenge<sup>23–25</sup>. To understand whether T cell metabolism in patients was linked to sorafenib responsiveness, we metabolically profiled their CD8<sup>+</sup> T cells by measuring the oxygen consumption rate (OCR; reflecting oxidative phosphorylation) and the extracellular acidification rate (ECAR; reflecting the rate of glycolysis indicated by lactate secretion) at baseline and during a mitochondrial fitness test<sup>23</sup>. In DLI-sorafenib responders, both the GC and SRC were significantly enhanced following sorafenib treatment (Fig. 6f,g and Supplementary Fig. 11b,c). In contrast, no changes in the metabolic profile were observed in DLI-sorafenib nonresponders following sorafenib treatment (Fig. 6h,i and Supplementary Fig. 11d,e).

The Shannon diversity indexes (DI) for the complementarity-determining region 3 (CDR3) amino acid sequences of the T cell receptor  $\alpha$  (TCR $\alpha$ ) and TCR $\beta$  chains were significantly higher in nonresponders than in responders (Fig. 6j). This was confirmed through analysis of variable gene segment usage for both TCR chains (Supplementary Fig. 12a,b). These observations are in line with previous studies showing that DLI response is linked to low diversity in the TCR repertoire<sup>26,27</sup>.

A retrospective analysis of 409 patients with FLT3-ITD<sup>+</sup> AML relapse after allo-HCT showed the dismal prognosis of these patients (Supplementary Fig. 13a–f and Supplementary Tables 1–11).

## DISCUSSION

Consistent with our data, results from others have shown that reduced IL-15 serum levels are associated with an increased risk for AML relapse after allo-HCT<sup>28</sup>. Graft-versus-leukemia (GVL) activity<sup>29,30</sup> as well as GVHD severity<sup>31–33</sup> increased upon administration of IL-15 after mouse allo-HCT. To avoid toxicity from a systemic increase in IL-15, we used sorafenib, which induces IL-15 production directly in the leukemia cell itself, thereby promoting a strong GVL effect without substantial induction of GVHD. In accordance with these findings, others have reported the production of IL-15 by acute leukemia cells<sup>34,35</sup>; however, no strategy has been developed to directly increase IL-15 production in malignant cells themselves. Our observation is highly relevant clinically, as the relapse rate in patients with FLT3-ITD<sup>+</sup> AML is 52% at 3 years after allo-HCT and the prognosis for these relapsed patients is poor<sup>36</sup>. We also explored the previous clinical observation of a synergistic effect between sorafenib and allo-HCT in FLT3-ITD<sup>+</sup> AML<sup>5</sup> through delineating the immunological mechanism underlying this observation, thereby providing a scientific rationale for using sorafenib to treat patients with relapsed FLT3-ITD<sup>+</sup> AML. In agreement with our results, it was shown that individuals receiving preemptive sorafenib treatment had lower relapse rates and improved survival as compared to a control group<sup>8–11</sup>.

Sorafenib-related IL-15 production improved the longevity phenotype of donor CD8<sup>+</sup> T cells and their ability to induce recall immunity. The increased GC and mitochondrial SRC of CD8<sup>+</sup> T cells from DLI-sorafenib responders with higher IL-15 serum levels are consistent with previous reports in CD8<sup>+</sup> T cells that indicate that IL-15

promotes mitochondrial biogenesis and contributes to enhanced glycolytic response following antigen challenge<sup>24</sup>.

Overall, we provide mouse and human data that support a new concept for treatment of FLT3-ITD<sup>+</sup> AML relapse following allo-HCT using sorafenib and DLI in combination. We show that FLT3 inhibition reduces ATF4 expression, allowing activation of the p-IRF7–IL-15 axis in leukemia cells. This in turn promotes immune memory against tumor cells, leading to immune-mediated cure of FLT3-ITD<sup>+</sup> AML relapse. A prospective study is required to determine whether the sorafenib–DLI combination is superior to other treatments.

## METHODS

Methods, including statements of data availability and any associated accession codes and references, are available in the [online version of the paper](#).

*Note: Any Supplementary Information and Source Data files are available in the online version of the paper.*

## ACKNOWLEDGMENTS

We thank G. Prinz and H. Dierbach for their help with mouse experiments, K. Geiger and D. Herchenbach for cell sorting, and S. Decker (University of Freiburg) for providing NSG mice. We thank M.E.D. Flowers (University of Washington) for help with patient data. We thank D. Cittaro for the help with bioinformatic analysis. *Il15*<sup>-/-</sup> mice were provided by Y. Tanriver (University of Freiburg). *Il15*<sup>-/-</sup> mice were provided by B. Becher (University of Zurich). This study was supported by the German Research Foundation (DFG) Heisenberg Professorship ZE 872/3-1 (R.Z.), DFG Sonderforschungsbereiche 1074 (SFB1074; F.K.), SFB1160 (R.Z.), SFB850 (T.B.), and TRR167 (R.Z.); European Research Council (ERC) Consolidator Grant no. 681012 GvHDCure (R.Z.); Deutsche Krebshilfe no. 111639 (G.H., R.Z.); Deutsche Jose Carreras Leukämie-Stiftung (DJCLS; G.H., R.Z.); Else Kröner-Fresenius Foundation (EKF) Stiftung no. 2015\_A147 (P.A.), INTERREG V Rhin Supérieur (P.A., R.Z.); LOEWE–Gentherapie Frankfurt (CGT), Hessian Ministry of Higher Education, Research and the Arts, Germany no. III L 4-518/17.004 (E.U.); Max-Eder-Nachwuchsgruppenprogramm, Deutsche Krebshilfe no. 109420 (F.K.); European Hematology Association fellowship 2010/04 (F.K.); and National Institutes of Health (NIH) grant no. R01 CA-72669 (B.R.B.). E.R. was supported by a fellowship from Associazione Italiana per la Ricerca sul Cancro (AIRC) that was cofunded by the European Union.

## AUTHOR CONTRIBUTIONS

N.R.M. performed the majority of the experiments, helped develop the overall concept behind the study, and helped write the manuscript. F.B. helped with the experiments and with development of the overall concept behind the study. L.B. performed ATF4 overexpression experiments. D.O.S. helped with Seahorse analysis. S. Thomas and S. Tugues helped with mouse experiments. M.W., T.A.M., K.H., P.A., A.L.I., G.I., K.S., W.M., S. Duquesne and A.W. helped with experiments and data interpretation. A.S.-G. performed immunohistological analysis. L.O. and K.-L.Y. helped with experiments. D.P., M.F., R. Claus, M. Lübbert, C.R., H. Bertz, R.W., J.H., A. Schmidts, M.S., D. Bettinger, R.T., E.U., Y.T., G.L.V., R.A., P.H., D. Wolf, M.D., C.J., K.W., C. Leiber, S. Gerull, J.H., C. Lengerke, T.P., T.S., G.K., W.R., S. Doostkam, S.M., and S.K.M. provided patient data. S. Taromi, S.S., and B.B. helped with mouse experiments. S.H. and T.B. helped with western blot and knockdown experiments. Z.H. and J. Dengjel performed mass spectrometry and data analysis. S.K. and B.K. performed mass spectrometry of sorafenib binding partners and kinase analysis. B.H., C. Schmid, U.H., C. Scheid, A. Spyridonidis, F.S., R.O., L.P.M., F.S.-d.-E., and J.K. provided patient data and helped with the analysis. M.P. performed analysis of the biopsy specimen. A.B., A. Nagler, D. Bunjes, A.M., W.H., and G.S. provided patient data and helped develop the overall concept behind the study. J.E.E. and D.F. analyzed the level of FLT3 inhibition upon sorafenib exposure. E.-M.W., J.-Y.C., F.K., D. Beelen, R. Chakraverty, S.R., S. Gill, N.K., F.A., L.V., J.S., and F.C. provided and analyzed patient data. E.R. and C.B. performed TRC sequencing and analyzed related data. A.M.M., T.K., T.T., B.K., D.K., D. Weisdorf, W.v.d.V., D.D., W.B., I.H., A.H., G.A., M. Bories, H. Busch, J.M., P.R., M. Labopin, J.H.A., A.S.H., G.R.H., G.A.K., M. Bar, A. Sarma, D.M., G.M., B.O., K.R., O.S., R.S.N., and A. Neubauer provided and analyzed patient data. E.U. and M.A.C. provided reagents and contributed to the development of the concept behind the study and the manuscript. B.R.B., N.v.B., and G.H. provided reagents, helped with the experiments, and analyzed data. E.P. helped to plan and analyze

the T cell metabolism experiments. J. Duyster and J.F. helped develop the concept behind the study, analyze the data, and write the manuscript. R.Z. developed the overall concept behind the study, supervised the experiments, analyzed the data, and wrote the manuscript.

## COMPETING FINANCIAL INTERESTS

The authors declare no competing financial interests.

Reprints and permissions information is available online at <http://www.nature.com/reprints/index.html>. Publisher's note: Springer Nature remains neutral with regard to jurisdictional claims in published maps and institutional affiliations.

- Pfirschmann, M. *et al.* Prediction of post-remission survival in acute myeloid leukaemia: a *post-hoc* analysis of the AML96 trial. *Lancet Oncol.* **13**, 207–214 (2012).
- Sengsayadeth, S.M. *et al.* Allo-SCT for high-risk AML-CR1 in the molecular era: impact of FLT3/ITD outweighs the conventional markers. *Bone Marrow Transplant.* **47**, 1535–1537 (2012).
- Serve, H. *et al.* Sorafenib in combination with intensive chemotherapy in elderly patients with acute myeloid leukemia: results from a randomized, placebo-controlled trial. *J. Clin. Oncol.* **31**, 3110–3118 (2013).
- Röllig, C. *et al.* Addition of sorafenib versus placebo to standard therapy in patients aged 60 years or younger with newly diagnosed acute myeloid leukaemia (SORAML): a multicentre, phase 2, randomised controlled trial. *Lancet Oncol.* **16**, 1691–1699 (2015).
- Metzelder, S.K. *et al.* High activity of sorafenib in FLT3-ITD-positive acute myeloid leukemia synergizes with allo-immune effects to induce sustained responses. *Leukemia* **26**, 2353–2359 (2012).
- Tschan-Plessl, A. *et al.* Synergistic effect of sorafenib and cGvHD in patients with high-risk FLT3-ITD<sup>+</sup> AML allows long-term disease control after allogeneic transplantation. *Ann. Hematol.* **94**, 1899–1905 (2015).
- Krüger, W.H. *et al.* Molecular remission of FLT3-ITD<sup>+</sup> AML relapse after allo-SCT by acute GVHD in addition to sorafenib. *Bone Marrow Transplant.* **47**, 137–138 (2012).
- Chen, Y.B. *et al.* Phase I trial of maintenance sorafenib after allogeneic hematopoietic stem cell transplantation for Fms-like tyrosine kinase 3 internal tandem duplication acute myeloid leukemia. *Biol. Blood Marrow Transplant.* **20**, 2042–2048 (2014).
- Antar, A., Kharfan-Dabaja, M.A., Mahfouz, R. & Bazarbachi, A. Sorafenib maintenance appears safe and improves clinical outcomes in FLT3-ITD acute myeloid leukemia after allogeneic hematopoietic cell transplantation. *Clin. Lymphoma Myeloma Leuk.* **15**, 298–302 (2015).
- Tarlock, K. *et al.* Sorafenib treatment following hematopoietic stem cell transplant in pediatric FLT3/ITD acute myeloid leukemia. *Pediatr. Blood Cancer* **62**, 1048–1054 (2015).
- Brunner, A.M. *et al.* Haematopoietic cell transplantation with and without sorafenib maintenance for patients with FLT3-ITD acute myeloid leukaemia in first complete remission. *Br. J. Haematol.* **175**, 496–504 (2016).
- Zorko, N.A. *et al.* *Mil* partial tandem duplication and *Fli3* internal tandem duplication in a double knock-in mouse recapitulates features of counterpart human acute myeloid leukemias. *Blood* **120**, 1130–1136 (2012).
- Bernot, K.M. *et al.* Eradicating acute myeloid leukemia in a *MIP<sup>TD</sup>/wt;Fli3<sup>TD</sup>/wt* murine model: a path to novel therapeutic approaches for human disease. *Blood* **122**, 3778–3783 (2013).
- Lucas, M., Schachterle, W., Oberle, K., Aichele, P. & Diefenbach, A. Dendritic cells prime natural killer cells by trans-presenting interleukin 15. *Immunity* **26**, 503–517 (2007).
- Rubio, V. *et al.* *Ex vivo* identification, isolation and analysis of tumor-cytolytic T cells. *Nat. Med.* **9**, 1377–1382 (2003).
- Pandiyani, P. *et al.* The role of IL-15 in activating STAT5 and fine-tuning IL-17A production in CD4 T lymphocytes. *J. Immunol.* **189**, 4237–4246 (2012).
- Patsoukis, N. *et al.* PD-1 alters T-cell metabolic reprogramming by inhibiting glycolysis and promoting lipolysis and fatty acid oxidation. *Nat. Commun.* **6**, 6692–6697 (2015).
- van Bockel, D.J. *et al.* Persistent survival of prevalent clonotypes within an immunodominant HIV gag-specific CD8<sup>+</sup> T cell response. *J. Immunol.* **186**, 359–371 (2011).
- Azimi, N., Shiramizu, K.M., Tagaya, Y., Mariner, J. & Waldmann, T.A. Viral activation of interleukin-15 (IL-15): characterization of a virus-inducible element in the IL-15 promoter region. *J. Virol.* **74**, 7338–7348 (2000).
- Romieu-Mourez, R. *et al.* Distinct roles for IFN regulatory factor (IRF)-3 and IRF-7 in the activation of antitumor properties of human macrophages. *Cancer Res.* **66**, 10576–10585 (2006).
- Liang, Q., Deng, H., Sun, C.W., Townes, T.M. & Zhu, F. Negative regulation of IRF7 activation by activating transcription factor 4 suggests a cross-regulation between the IFN responses and the cellular integrated stress responses. *J. Immunol.* **186**, 1001–1010 (2011).
- Smith, C.C., Lin, K., Stecula, A., Sali, A. & Shah, N.P. *FLT3* D835 mutations confer differential resistance to type II *FLT3* inhibitors. *Leukemia* **29**, 2390–2392 (2015).
- Buck, M.D., O'Sullivan, D. & Pearce, E.L. T cell metabolism drives immunity. *J. Exp. Med.* **212**, 1345–1360 (2015).
- van der Windt, G.J. *et al.* Mitochondrial respiratory capacity is a critical regulator of CD8<sup>+</sup> T cell memory development. *Immunity* **36**, 68–78 (2012).
- van der Windt, G.J. *et al.* CD8 memory T cells have a bioenergetic advantage that underlies their rapid recall ability. *Proc. Natl. Acad. Sci. USA* **110**, 14336–14341 (2013).
- Schultze-Florey, C. *et al.* TCR diversity is a predictive marker for donor lymphocyte infusion response. *Blood* **128**, 4605 (2016).
- van Bergen, C.A. *et al.* Selective graft-versus-leukemia depends on magnitude and diversity of the alloreactive T cell response. *J. Clin. Invest.* **127**, 517–529 (2017).
- Thiant, S. *et al.* Plasma levels of IL-7 and IL-15 in the first month after myeloablative BMT are predictive biomarkers of both acute GVHD and relapse. *Bone Marrow Transplant.* **45**, 1546–1552 (2010).
- Sauter, C.T. *et al.* Interleukin-15 administration increases graft-versus-tumor activity in recipients of haploidentical hematopoietic SCT. *Bone Marrow Transplant.* **48**, 1237–1242 (2013).
- Chen, G. *et al.* Expanded donor natural killer cell and IL-2, IL-15 treatment efficacy in allogeneic hematopoietic stem cell transplantation. *Eur. J. Haematol.* **81**, 226–235 (2008).
- Blaser, B.W. *et al.* Donor-derived IL-15 is critical for acute allogeneic graft-versus-host disease. *Blood* **105**, 894–901 (2005).
- Blaser, B.W. *et al.* Trans-presentation of donor-derived interleukin 15 is necessary for the rapid onset of acute graft-versus-host disease but not for graft-versus-tumor activity. *Blood* **108**, 2463–2469 (2006).
- Roychowdhury, S. *et al.* IL-15 but not IL-2 rapidly induces lethal xenogeneic graft-versus-host disease. *Blood* **106**, 2433–2435 (2005).
- Cario, G. *et al.* High interleukin-15 expression characterizes childhood acute lymphoblastic leukemia with involvement of the CNS. *J. Clin. Oncol.* **25**, 4813–4820 (2007).
- Wu, S. *et al.* Expression of interleukin 15 in primary adult acute lymphoblastic leukemia. *Cancer* **116**, 387–392 (2010).
- Nasilowska-Adamska, B. *et al.* Mild chronic graft-versus-host disease may alleviate poor prognosis associated with *FLT3* internal tandem duplication for adult acute myeloid leukemia following allogeneic stem cell transplantation with myeloablative conditioning in first complete remission: a retrospective study. *Eur. J. Haematol.* **96**, 236–244 (2016).
- Barnes, B.J., Moore, P.A. & Pittha, P.M. Virus-specific activation of a novel interferon regulatory factor, IRF-5, results in the induction of distinct interferon  $\alpha$  genes. *J. Biol. Chem.* **276**, 23382–23390 (2001).

Nimitha R Mathew<sup>1,2</sup>, Francis Baumgartner<sup>1</sup>, Lukas Braun<sup>1</sup>, David O'Sullivan<sup>3</sup>, Simone Thomas<sup>4</sup>, Miguel Waterhouse<sup>1</sup>, Tony A Müller<sup>1</sup>, Kathrin Hanke<sup>1,2</sup>, Sanaz Taromi<sup>1</sup>, Petya Apostolova<sup>1</sup>, Anna L Illert<sup>1</sup>, Wolfgang Melchinger<sup>1</sup>, Sandra Duquesne<sup>1</sup>, Annette Schmitt-Graeff<sup>5</sup>, Lena Osswald<sup>1</sup>, Kai-Li Yan<sup>1</sup>, Arnim Weber<sup>6</sup>, Sonia Tugues<sup>7</sup>, Sabine Spath<sup>7</sup>, Dietmar Pfeifer<sup>1</sup>, Marie Follo<sup>1</sup>, Rainer Claus<sup>1</sup>, Michael Lübbert<sup>1</sup>, Christoph Rummelt<sup>1</sup>, Hartmut Bertz<sup>1</sup>, Ralph Wäsch<sup>1</sup>, Johanna Haag<sup>1</sup>, Andrea Schmidts<sup>1</sup>, Michael Schultheiss<sup>8</sup>, Dominik Bettinger<sup>8</sup>, Robert Thimme<sup>8</sup>, Evelyn Ullrich<sup>9</sup>, Yakup Tanriver<sup>6,10</sup>, Giang Lam Vuong<sup>11</sup>, Renate Arnold<sup>11</sup>, Philipp Hemmati<sup>11</sup>, Dominik Wolf<sup>12,13</sup>, Markus Ditschkowski<sup>14</sup>, Cordula Jilg<sup>15</sup>, Konrad Wilhelm<sup>15</sup>, Christian Leiber<sup>15</sup>, Sabine Gerull<sup>16</sup>, Jörg Halter<sup>16</sup>, Claudia Lengerke<sup>16</sup>, Thomas Pabst<sup>17</sup>, Thomas Schroeder<sup>18</sup>, Guido Kobbe<sup>18</sup>, Wolf Rösler<sup>19</sup>, Soroush Doostkam<sup>20</sup>, Stephan Meckel<sup>21</sup>, Kathleen Stabla<sup>22,23</sup>, Stephan K Metzelder<sup>22,23</sup>, Sebastian Halbach<sup>24</sup>, Tilman Brummer<sup>24–27</sup>, Zehan Hu<sup>28,29</sup>, Joern Dengjel<sup>28,29</sup>, Björn Hackanson<sup>30</sup>, Christoph Schmid<sup>30</sup>, Udo Holtick<sup>31</sup>, Christof Scheid<sup>31</sup>, Alexandros Spyridonidis<sup>32</sup>, Friedrich Stölzel<sup>33</sup>, Rainer Ordemann<sup>33</sup>, Lutz P Müller<sup>34</sup>, Flore Sicre-de-Fontbrune<sup>35,36</sup>, Gabriele Ihorst<sup>37</sup>, Jürgen Kuball<sup>38</sup>, Jan E Ehlert<sup>39</sup>, Daniel Feger<sup>39</sup>, Eva-Maria Wagner<sup>40</sup>, Jean-Yves Cahn<sup>41</sup>,

Jacqueline Schnell<sup>42</sup>, Florian Kuchenbauer<sup>42</sup>, Donald Bunjes<sup>42</sup>, Ronjon Chakraverty<sup>43,44</sup>, Simon Richardson<sup>43,44</sup>, Saar Gill<sup>45</sup>, Nicolaus Kröger<sup>46</sup>, Francis Ayuk<sup>46</sup>, Luca Vago<sup>47–49</sup>, Fabio Ciceri<sup>47–49</sup>, Antonia M Müller<sup>50</sup>, Takeshi Kondo<sup>51</sup>, Takanori Teshima<sup>51</sup> , Susan Klaeger<sup>27,52</sup>, Bernhard Kuster<sup>52</sup> , Dennis (Dong Hwan) Kim<sup>53</sup>, Daniel Weisdorf<sup>54</sup>, Walter van der Velden<sup>55</sup>, Daniela Dörfel<sup>56</sup>, Wolfgang Bethge<sup>56</sup>, Inken Hilgendorf<sup>57</sup>, Andreas Hochhaus<sup>57</sup>, Geoffroy Andrieux<sup>25,27,58</sup>, Melanie Börries<sup>25,27,58</sup>, Hauke Busch<sup>25,27,58,59</sup> , John Magenau<sup>60</sup>, Pavan Reddy<sup>60</sup>, Myriam Labopin<sup>61</sup>, Joseph H Antin<sup>62</sup>, Andrea S Henden<sup>63,64</sup>, Geoffrey R Hill<sup>63–65</sup>, Glen A Kennedy<sup>65</sup>, Merav Bar<sup>66</sup>, Anita Sarma<sup>67</sup>, Donal McLornan<sup>67</sup>, Ghulam Mufti<sup>67</sup>, Betul Oran<sup>68</sup>, Katayoun Rezvani<sup>68</sup>, Omid Shah<sup>69</sup>, Robert S Negrin<sup>69</sup>, Arnon Nagler<sup>70</sup>, Marco Prinz<sup>21,26</sup>, Andreas Burchert<sup>24</sup>, Andreas Neubauer<sup>22,23</sup>, Dietrich Beelen<sup>15</sup>, Andreas Mackensen<sup>20</sup> , Nikolas von Bubnoff<sup>1</sup>, Wolfgang Herr<sup>4</sup>, Burkhard Becher<sup>7</sup> , Gerard Socie<sup>35,36</sup>, Michael A Caligiuri<sup>71</sup>, Eliana Ruggiero<sup>47–49</sup>, Chiara Bonini<sup>47–49</sup>, Georg Häcker<sup>6</sup>, Justus Duyster<sup>1</sup>, Jürgen Finke<sup>1</sup>, Erika Pearce<sup>3</sup>, Bruce R Blazar<sup>72</sup> & Robert Zeiser<sup>1,26</sup>

<sup>1</sup>Department of Hematology, Oncology and Stem Cell Transplantation, Faculty of Medicine, University Medical Center Freiburg, University of Freiburg, Freiburg, Germany. <sup>2</sup>Faculty of Biology, University of Freiburg, Freiburg, Germany. <sup>3</sup>Max Planck Institute for Immunobiology and Epigenetics, Freiburg, Germany. <sup>4</sup>Department of Internal Medicine III, Hematology and Oncology, University Hospital Regensburg, Regensburg, Germany. <sup>5</sup>Department of Pathology, University Medical Center Freiburg, University of Freiburg, Freiburg, Germany. <sup>6</sup>Department of Medical Microbiology and Hygiene, University Medical Center Freiburg, University of Freiburg, Freiburg, Germany. <sup>7</sup>Institute of Experimental Immunology, University of Zurich, Zurich, Switzerland. <sup>8</sup>Department of Medicine II, Faculty of Medicine, University Medical Center Freiburg, University of Freiburg, Freiburg, Germany. <sup>9</sup>Department for Children and Adolescents Medicine, Division of Stem Cell Transplantation and Immunology, University Hospital Frankfurt, Goethe University Frankfurt, Frankfurt, Germany. <sup>10</sup>Department of Nephrology, University Medical Center Freiburg, University of Freiburg, Freiburg, Germany. <sup>11</sup>Department of Stem Cell Transplantation, Charité University Medicine Berlin, Berlin, Germany. <sup>12</sup>Medical Clinic III, Oncology, Hematology, Immunooncology and Rheumatology, University Hospital Bonn (UKB), Bonn, Germany. <sup>13</sup>Department of Hematology, University Medical Center Innsbruck, Austria. <sup>14</sup>Department of Bone Marrow Transplantation, West German Cancer Center, University Hospital Essen, Essen, Germany. <sup>15</sup>Department of Urology, University Medical Center Freiburg, University of Freiburg, Freiburg, Germany. <sup>16</sup>Division of Hematology, University Hospital Basel, Basel, Switzerland. <sup>17</sup>Department of Internal Medicine, Inselspital/Universitätsspital Bern, Bern, Switzerland. <sup>18</sup>Department of Hematology, Oncology and Clinical Immunology, Universitätsklinikum, Düsseldorf, Düsseldorf, Germany. <sup>19</sup>Department of Hematology and Oncology, University of Erlangen, Erlangen, Germany. <sup>20</sup>Institute for Neuropathology, University of Freiburg, Freiburg, Germany. <sup>21</sup>Department of Neuroradiology, University Medical Center Freiburg, University of Freiburg, Freiburg, Germany. <sup>22</sup>Department of Hematology, Oncology and Immunology, Philipps University Marburg, Marburg, Germany. <sup>23</sup>Department of Hematology, University Hospital of Giessen and Marburg, Marburg, Germany. <sup>24</sup>Institute of Molecular Medicine and Cell Research (IMMZ), Faculty of Medicine, University Medical Center Freiburg, University of Freiburg, Freiburg, Germany. <sup>25</sup>German Cancer Consortium (DKTK), Partner Site Freiburg, Freiburg, Germany. <sup>26</sup>Center for Biological Signaling Studies (BIOSS), University of Freiburg, Freiburg, Germany. <sup>27</sup>German Cancer Research Center (DKFZ), Heidelberg, Germany. <sup>28</sup>Department of Dermatology, University Medical Center, University of Freiburg, Freiburg, Germany. <sup>29</sup>Department of Biology, University of Fribourg, Fribourg, Switzerland. <sup>30</sup>Interdisciplinary Cancer Center Augsburg (ICCA) II, Clinic for Internal Medicine, Augsburg, Germany. <sup>31</sup>Department of Internal Medicine I, University Hospital Cologne, Cologne, Germany. <sup>32</sup>Hematology Stem Cell Transplant Unit, School of Medicine, University of Patras, Patras, Greece. <sup>33</sup>Department of Hematology and Oncology, Universitätsklinikum Carl Gustav Carus and Technischen Universität Dresden, Dresden, Germany. <sup>34</sup>Department of Hematology and Oncology, Universitätsklinikum Halle, Halle, Germany. <sup>35</sup>Assistance Publique—Hôpitaux de Paris, Hematology Stem Cell Transplantation, Saint Louis Hospital, Paris, France. <sup>36</sup>INSERM UMR 1160, Paris, France. <sup>37</sup>Clinical Trials Unit, Faculty of Medicine, University Medical Center, University of Freiburg, Freiburg, Germany. <sup>38</sup>Department of Hematology, University Medical Center Utrecht, Utrecht, the Netherlands. <sup>39</sup>ProQinase, Freiburg, Germany. <sup>40</sup>Department of Hematology and Oncology, Universitätsmedizin Mainz, Mainz, Germany. <sup>41</sup>Clinique Universitaire Hématologie, Université Grenoble Alpes, Grenoble, France. <sup>42</sup>Department of Internal Medicine III, University Hospital of Ulm, Ulm, Germany. <sup>43</sup>Cancer Institute, Royal Free Hospital, London, UK. <sup>44</sup>Institute of Immunity and Transplantation, Royal Free Hospital, London, UK. <sup>45</sup>Smilow Translational Research Center, Hospital of the University of Pennsylvania, Philadelphia, Pennsylvania, USA. <sup>46</sup>Department of Stem Cell Transplantation, University Hospital Hamburg-Eppendorf, Hamburg, Germany. <sup>47</sup>Unit of Immunogenetics, Leukemia Genomics and Immunobiology, San Raffaele Scientific Institute, Milan, Italy. <sup>48</sup>Unit of Hematology and Bone Marrow Transplantation, San Raffaele Scientific Institute, Milan, Italy. <sup>49</sup>Department of Hematology, University Vita-Salute, San Raffaele University, Milan, Italy. <sup>50</sup>Department of Hematology, University Hospital Zurich, Zurich, Switzerland. <sup>51</sup>Department of Hematology, Hokkaido University, Sapporo, Japan. <sup>52</sup>Proteomics and Bioanalytics, Technische Universität München, Partner Site of the German Cancer Consortium, Freising, Germany. <sup>53</sup>Department of Medical Oncology & Hematology, Princess Margaret Cancer Centre, University of Toronto, Toronto, Ontario, Canada. <sup>54</sup>Hematology, Oncology and Transplantation, University of Minnesota, Minneapolis, Minnesota, USA. <sup>55</sup>Department of Hematology, Radboud University, Nijmegen, the Netherlands. <sup>56</sup>Medizinische Klinik II, Universitätsklinikum Tübingen, Tübingen, Germany. <sup>57</sup>Klinik für Innere Medizin II, Universitätsklinikum Jena, Jena, Germany. <sup>58</sup>Systems Biology of the Cellular Microenvironment Group, IMMZ, ALU, Freiburg, Germany. <sup>59</sup>Institute of Experimental Dermatology, University of Lübeck, Lübeck, Germany. <sup>60</sup>Department of Hematology, University of Michigan Medical School, Ann Arbor, Michigan, USA. <sup>61</sup>EBMT Statistical Unit, Hôpital Saint Antoine Paris, Paris, France. <sup>62</sup>Dana-Farber Cancer Institute, Harvard Medical School, Harvard University, Boston, Massachusetts, USA. <sup>63</sup>Bone Marrow Transplant Laboratory, QIMR Berghofer Medical Research Institute, Brisbane, Queensland, Australia. <sup>64</sup>Department of Haematology, Royal Brisbane Hospital, Brisbane, Queensland, Australia. <sup>65</sup>Department of Haematology, Royal Brisbane and Womens Hospital, Brisbane, Queensland, Australia. <sup>66</sup>Division of Blood and Marrow Transplantation, Fred Hutchinson Cancer Research Center, University of Washington, Seattle, Washington, USA. <sup>67</sup>Department of Haematological Medicine, King's College Hospital NHS Foundation Trust, London, UK. <sup>68</sup>Division of Bone Marrow Transplantation, MD Anderson Cancer Center, Houston, Texas, USA. <sup>69</sup>Division of Blood and Marrow Transplantation, Stanford University Medical School, Stanford, California, USA. <sup>70</sup>Division of Hematology, Chaim Sheba Medical Center, Tel Hashomer, Israel. <sup>71</sup>Ohio State University Comprehensive Cancer Center, Ohio State University, Columbus, Ohio, USA. <sup>72</sup>Department of Pediatrics, Division of Blood and Marrow Transplantation, University of Minnesota, Minneapolis, Minnesota, USA. Correspondence should be addressed to R.Z. ([robert.zeiser@uniklinik-freiburg.de](mailto:robert.zeiser@uniklinik-freiburg.de)).

## ONLINE METHODS

**Human subjects.** Protocols for human sample collection and analysis were approved by the Institutional Ethics Review Board (IRB) of the Medical Center at the University of Freiburg, Germany (Protocol numbers: 10024/13, 26/11, 509/16 “Analysis of patients with FLT3-ITD-mutated AML after allogeneic hematopoietic cell transplantation”), and the study was registered at ClinicalTrials.gov (NCT02867891). Written informed consent was obtained from each patient. All analyses of human data were carried out in compliance with the relevant ethical regulations.

With IRB approval, we conducted a multicenter, retrospective analysis of patients with FLT3-ITD<sup>+</sup> AML who received any kind of therapy for hematological relapse after allo-HCT. We contacted the transplant programs with the highest volumes of patients with AML undergoing allo-HCT, which were provided by the European Group for Blood and Marrow Transplantation (EBMT). Additional sites in the United States, Canada, Japan, and Australia were surveyed on the basis of recommendation from these initial sites.

All data reported by the transplant centers is shown in **Supplementary Table 1**. Of the 419 patients with relapse of FLT3-ITD<sup>+</sup> AML after allo-HCT, 10 patients were excluded because they received no relapse treatment ( $n = 6$ ), they had no hematological relapse ( $n = 1$ ), their survival data were incomplete ( $n = 1$ ), the time until second allo-HCT was unknown ( $n = 1$ ), or they never entered remission after allo-HCT ( $n = 1$ ). All excluded patients are displayed in **Supplementary Table 1**. The resulting 409 patients with FLT3-ITD<sup>+</sup> AML relapse after allo-HCT were analyzed for response rates and OS.

The decision to treat relapse was made by the individual centers on the basis of published literature providing a scientific rationale for DLI<sup>38–40</sup> and DLI combined with sorafenib<sup>5</sup>. To date, no international guidelines or clinical pathway recommendations exist specifically for patients who relapse with FLT3-ITD<sup>+</sup> AML after allo-HCT. Sorafenib was given at a dosage of 400 mg twice daily.

The patients' characteristics, including age at treatment and sex, AML characteristics, donor type, conditioning regimen, immunosuppressive regimen, and remission status before transplant, are detailed in **Supplementary Table 1** for each patient. The data for each treatment group are summarized in **Supplementary Tables 2–11**.

**Mice.** C57BL/6 (H-2Kb, Thy-1.2), BALB/c (H-2Kd, Thy-1.2), NSG, and *Rag2<sup>-/-</sup>Il2ra<sup>-/-</sup>* mice were purchased from Charles River Laboratory (Sulzfeld, Germany) or Janvier Labs (France) or were taken from the local stock at the animal facility at the University of Freiburg. *Il15<sup>-/-</sup>* mice were provided by Y. Tanriver (University of Freiburg). *Il15ra<sup>-/-</sup>* mice were provided by B. Becher (University of Zurich). Mice were between 6 and 12 weeks of age at the time of the experiments, and donor–recipient pairs that were both female or both male were used. Mouse experiments were carried out in compliance with relevant animal-use guidelines and ethical regulations. Protocols for mouse experiments (Protocol numbers: G13-116, G-15/018, G-16/018, G-17/093) were approved by the Regierungspräsidium (Federal Ministry for Nature, Environment and Consumers' Protection) Freiburg, Freiburg, Germany.

**Immunologic analysis.** Correlative studies were performed before sorafenib treatment (day -3, day -2 or day 0 relative to start of sorafenib as indicated in the figure; day 0 was prior to sorafenib treatment but within the same day as start of sorafenib treatment) and on different days after the start of sorafenib treatment, as indicated in the figure legends. These studies included the following: immunophenotypic analysis of peripheral blood mononuclear cells (PBMCs) using flow cytometry; immunohistochemical staining of formalin-fixed, paraffin-embedded BM biopsy specimens; whole-exome sequencing of enriched AML cells; DNA sequencing of the TCR chains of enriched T cells; analysis of CD8<sup>+</sup> T cell metabolism; microarray analysis of enriched AML cells; and cytokine and chemokine assays of plasma samples.

**Metabolism assays (Seahorse) of human CD8<sup>+</sup> T cells.** The OCR and ECAR of human CD8<sup>+</sup> T cells were measured in XF medium (nonbuffered RPMI-1640 containing 25 mM glucose, 2 mM L-glutamine, and 1 mM sodium pyruvate) under basal conditions and in response to 1 μM oligomycin, 1.5 μM carbonyl cyanide-4-(trifluoromethoxy)phenylhydrazone (FCCP), and 100 nM rotenone

+ 1 μM antimycin A (all from Sigma) using a 96-well XFe Extracellular Flux Analyzer (Seahorse Bioscience) as previously described<sup>41</sup>.

**Whole-genome sequencing.** Whole-genome sequencing was performed for four tumor samples on the Illumina HiSeq X platform. Each sample was sequenced on four lanes to ensure good coverage. After trimming of poor-quality reads<sup>42</sup>, reads were aligned to the hg19 human reference genome using Burrows–Wheeler aligner (BWA)<sup>43</sup>. Duplicate removal, indel realignment, and base-quality recalibration were performed using the Genome Analysis Toolkit<sup>44</sup>. We called SNP and indel mutations and applied false-positive filtering using VarScan 2. Relevant mutations were selected using the following criteria: read depth >8 reads per base, variant allele frequency >9%, and minor allele frequency (MAF) from the Exome Aggregation Consortium (ExAC) database<sup>45</sup> <0.1%. Copy number alteration analysis was performed using Control-FREEC<sup>46</sup>.

**Gene expression analysis of responder and nonresponder patients after sorafenib treatment.** RNA was extracted from PBMCs isolated from 8 ml of blood in eight patients. The blood was isolated from the same patient 3 d before start of sorafenib and 6 d after the start of sorafenib. For each sample, 2 μg of total RNA from ~10<sup>7</sup> cells was incubated with DNase I according to the manufacturer's instructions (Qiagen, Germany) and was cleaned up using the RNeasy Micro Kit (Qiagen, Germany). RNA integrity was analyzed by capillary electrophoresis using a Fragment Analyzer (Advanced Analytical Technologies, Inc., Ames, IA). RNA samples were further processed with the Affymetrix GeneChip Pico kit and hybridized to Affymetrix Clariom S arrays as described by the manufacturer (Affymetrix, USA). The arrays were normalized via robust multichip averaging as implemented in the R/Bioconductor oligo package<sup>47</sup>. Gene set enrichment was calculated using the R/Bioconductor package gage<sup>48</sup> with the pathways from ConsensusPathDB<sup>49</sup> as gene sets and a significance cutoff of  $P < 0.05$ .

**Overexpression of ATF4 in Ba/F3-ITD cells.** The lentiviral vector for overexpression of mouse ATF4, mATF4 (Plasmid no. 24874), was purchased from Addgene, USA. The 293T cell line used for packaging was purchased from Clontech, France, and cultured in DMEM, high glucose supplemented with GlutaMAX, pyruvate (Gibco, Germany), 10% FCS (PAN-Biotech, Germany), and 1% penicillin–streptomycin (Gibco, Germany). The packaging cells were transiently transfected with 10 μg of mATF4 and 10 μg of envelope vector pVSV-G using CaCl<sub>2</sub>, and viral stocks were collected 48 and 72 h after transfection. We used these viral stocks to transduce Ba/F3-ITD cells, and the cells were cultured in 2 μg/ml puromycin (Invivogen, France) for selection of transduced cells. The overexpression of ATF4 in puromycin-selected cells was confirmed by western blotting.

**Knockdown of IRF7 in MOLM-13 cells.** HEK293T packaging cells were cultured as described previously<sup>50</sup>. Doxycycline-inducible lentiviral vectors, pTRIPZ-inducible lentiviral human *IRF7*-targeted shRNA (clone ID: V3THS\_356931) and pTRIPZ-inducible lentiviral nonsilencing (NS) shRNA control (no. RHS4743) with a turboRFP reporter, were purchased from Dharmacon, Germany. Lentiviral particles were generated by transfection of HEK293T cells using polyethylenimine (Polysciences) and the Trans-Lentiviral Packaging System (Dharmacon, Germany). 5 × 10<sup>5</sup> MOLM-13 cells were transduced with the lentiviral particles (transfected cells are annotated as MOLM-13<sup>NS shRNA</sup> and MOLM-13<sup>IRF7 shRNA</sup>). The cells were selected in 2 μg/ml puromycin (Invivogen, Germany) starting at 24 h after infection. The cells were cultured in medium containing 2 μg/ml doxycycline for 11 d to induce expression of the shRNA. Knockdown of IRF7 was confirmed by western blotting.

**Bone marrow transplantation model and histopathology scoring.** BM transplantation experiments were performed as previously described<sup>51,52</sup>. Briefly, recipients were i.v. injected with 5 × 10<sup>6</sup> WT BM cells after lethal irradiation using 9–11 Gy. To induce GVHD, CD4<sup>+</sup> and CD8<sup>+</sup> T cells were isolated from donor spleens and enriched through positive selection with the magnetic-activation cell sorting (MACS) system (Miltenyi Biotec, USA) according to the manufacturer's instructions. Anti-CD4 and anti-CD8 MicroBeads were used. CD4<sup>+</sup> and CD8<sup>+</sup> T cell purity was at least 90% as assessed by flow

cytometry (data not shown). CD4<sup>+</sup> and CD8<sup>+</sup> T cells were injected at a dosage of  $2 \times 10^5$  (C57BL/6-derived) or  $5 \times 10^5$  (BALB/c-derived) cells i.v. on day 2 following the transplantation of BM cells with or without leukemia cells. Slides of small intestine, large intestine, and liver specimens collected after allo-HCT were stained with H&E and scored by an experienced pathologist blinded to the identity of treatment groups. GVHD severity was determined according to a previously published histopathology scoring system<sup>53</sup>.

**Depletion of NK cells.** To deplete NK cells, BM was stained for CD3 and NK1.1 surface markers. BM was depleted of NK1.1<sup>+</sup>CD3<sup>-</sup> cells using FACS sorting by excluding all NK1.1<sup>+</sup>CD3<sup>-</sup> cells.

**qPCR for IL-15 expression from mouse and human cells.** Mouse Ba/F3-ITD cells were treated with DMSO or different concentrations of sorafenib, tandutinib, crenolanib, midostaurin, or quizartinib for 24 h as indicated in the figure legends. Total RNA was isolated using the miRNeasy Mini Kit (Qiagen, Netherlands) or QIAzol lysis reagent (Qiagen, Netherlands) according to the manufacturer's instructions. 1 µg of total RNA from treated Ba/F3-ITD cells was reverse transcribed into cDNA using the high-capacity cDNA Reverse Transcription Kit (Thermo Scientific, USA). qPCR was carried out using the LightCycler 480 SYBR Green I Master kit (Roche, Switzerland) in a LightCycler 480 instrument (Roche, Switzerland). 50–80 ng cDNA was used for qPCR analysis. For analysis of mouse *Il15* mRNA expression by Ba/F3-ITD cells, primers (sense primer: 5'-CATCCATCTCGTGCTACTT-3', antisense primer: 5'-TTCTCCAGGTCATATCTTACAT-3') were designed using Beacon Designer software (Premier Biosoft, UK) and were synthesized by Apar Biosciences, Germany. The reference gene was selected using the Primer Only geNorm 12-gene kit for use with SYBR Green (ge-SY-12, PrimerDesign, UK) and geNorm analysis software (PrimerDesign, USA) according to the manufacturer's instructions. *Il15* mRNA expression was normalized to that of the reference gene *Mon2*. Mouse *Il15* primers were synthesized by and purchased from Apar Biosciences, Germany, whereas *Mon2* primers were purchased from PrimerDesign, USA.

For analysis of human *IL15* mRNA expression, MV-411, MOLM-13<sup>NS shRNA</sup>, MOLM-13<sup>IRF7 shRNA</sup>, HL60, NB4, and U937 cells and human PBMCs were treated with DMSO or different concentrations of sorafenib, quizartinib, or tandutinib for 24 or 48 h as indicated in the figure legends. Cells were harvested and lysed in QIAzol lysis reagent (Qiagen, Netherlands), and total RNA was isolated according to the manufacturer's instructions. 300 ng–1 µg of total RNA was reverse transcribed into cDNA using the High-Capacity cDNA Reverse Transcription Kit (Thermo Scientific, USA). qPCR was carried out using the LightCycler 480 SYBR Green I Master kit (Roche, Switzerland) in a LightCycler 480 instrument (Roche, Switzerland). 50 ng cDNA was used for qPCR analysis. The RT-qPCR<sup>2</sup> Primer Assay for Human IL-15 (Qiagen, Netherlands) was used for detecting human *IL15* mRNA expression. The reference gene was selected using the Primer Only geNorm 12-gene kit for use with SYBR Green (ge-SY-12, PrimerDesign, UK) and the geNorm analysis software (PrimerDesign, USA) according to the manufacturer's instruction. *GAPDH* was used as the reference gene (sense primer: 5'-CTCCTCCACCTTGGACGCTG-3', antisense primer: 5'-ACCACCCTGTTGCTGTAGCC-3') for untreated human PBMCs or human PBMCs treated with DMSO or sorafenib and for MV4-11 cells treated with DMSO or different concentrations of tandutinib or quizartinib. Human *GAPDH* primers were synthesized by and purchased from Apar Bioscience, Germany, or Eurofins Genomics, Germany. *ENOX2* was used as the reference gene for MOLM-13<sup>NS shRNA</sup> cells and MOLM-13<sup>IRF7 shRNA</sup> cells, which were treated with DMSO or different concentrations of sorafenib. *ENOX2* primers were purchased from PrimerDesign, USA.

**Flow cytometry.** All antibodies used for flow cytometry are listed in **Supplementary Table 12**. For all fluorochrome-conjugated antibodies, optimal concentrations were determined using titration experiments. Cells were incubated with the respective antibodies diluted in FACS buffer for 20 min at 4 °C for surface antigen staining. Cells were then washed with FACS buffer according to the manufacturer's instructions. For mouse p-STAT5 analysis, cells were fixed with one part prewarmed 3.7% formalin and one part FACS buffer and then were exposed to 90% methanol before the p-STAT5 antibody was added. All intracellular cytokine stainings were performed using the BD Cytofix/Cytoperm kit (BD

Biosciences, Germany). For intracellular cytokine staining for mouse IFN-γ, before staining, cells were restimulated with 0.5 µg/ml phorbol 12-myristate 13-acetate (PMA, Sigma-Aldrich, Germany) and 50 ng/ml ionomycin (Sigma-Aldrich, Germany) for 5 h, and medium containing 1 µl/ml brefeldin A (Golgi Plug, BD Biosciences, Germany) was added 2 h into restimulation. For intracellular staining of IL-15, cells were treated with medium containing 1 µl/ml brefeldin A (Golgi Plug, BD Biosciences, Germany) for 8 h before staining with unconjugated anti-IL-15 antibody (overnight staining at 4 °C). The cells were then stained with allophycocyanin (APC)-conjugated F(ab')<sub>2</sub> anti-rat IgG secondary antibody (polyclonal antibody, catalog number 17-4010-82, eBioscience, Germany). For intracellular staining of human IFN-γ and perforin, cells were fixed with 4% paraformaldehyde and stained in 1× BD Perm/Wash Buffer according to the manufacturer's instructions. To exclude dead cells, the LIVE/DEAD Fixable Dead Cell Stain Kit (Molecular Probes, USA) was used according to the manufacturer's instructions. Data were acquired on a BD LSR Fortessa (BD Biosciences, Germany) or Flow Cytometer CyAn ADP (Beckman Coulter, Germany) and analyzed using FlowJo software (Tree Star, USA). The gating strategy is provided in **Supplementary Figure 14**.

**Statistical analysis.** For the sample size in the mouse GVL survival experiments, a power analysis was performed. A sample size of at least  $n = 8$  mice per group was determined by 80% power to reach statistical significance of 0.05 to detect an effect size of at least 1.06. For the xenograft model,  $n = 7$  mice per group was used because of the greater differences expected in this experimental setting. Differences in animal survival (Kaplan–Meier survival curves) were analyzed using the Mantel–Cox test. The experiments were performed in a nonblinded fashion, except for the GVHD severity scoring. To obtain unbiased data, the histopathological scoring of GVHD severity was performed by a pathologist blinded to both the genotype and treatment group. After finalization of the quantitative GVHD severity scores, the samples were allocated to their genotypes and treatment groups. There was no randomization of mice or samples before analysis. All samples and mice were included in our analyses.

For statistical analysis, an unpaired Student's *t*-test (two-sided) was applied. All data were tested for normality through applying the Kolmogorov–Smirnov test. If data did not meet the criteria of normality, the Mann–Whitney *U* test was applied. The Wilcoxon matched-pairs signed-rank test was used to analyze related samples. Data are presented as mean ± s.e.m. (error bars). Differences were considered significant when the *P* value was <0.05.

Patient data were analyzed using SAS 9.2 (SAS Institute, Inc., Cary, NC, USA). OS was calculated as the time from the start of treatment until the date of death from any cause. Patients alive at the end of the observation period were censored at the time they were last seen alive. OS rates and median survival times were estimated using the Kaplan–Meier method.

**Other methods.** All other methods are described in the **Supplementary Note**.

**Life Sciences Reporting Summary.** Further information on experimental design and reagents is available in the **Life Sciences Reporting Summary**.

**Data availability.** Microarrays: GEO accession number, [GSE95770](#); ArrayExpress accession number, [E-MTAB-4487](#). All data are available from the authors upon reasonable request. Uncut western blots are displayed in **Supplementary Figures 15–21**.

- Steinmann, J. *et al.* 5-Azacytidine and DLI can induce long-term remissions in AML patients relapsed after allograft. *Bone Marrow Transplant.* **50**, 690–695 (2015).
- Bejanyan, N. *et al.* Survival of patients with acute myeloid leukemia relapsing after allogeneic hematopoietic cell transplantation: a center for international blood and marrow transplant research study. *Biol. Blood Marrow Transplant.* **21**, 454–459 (2015).
- Takami, A. *et al.* Donor lymphocyte infusion for the treatment of relapsed acute myeloid leukemia after allogeneic hematopoietic stem cell transplantation: a retrospective analysis by the Adult Acute Myeloid Leukemia Working Group of the Japan Society for Hematopoietic Cell Transplantation. *Biol. Blood Marrow Transplant.* **20**, 1785–1790 (2014).
- Buck, M.D. *et al.* Mitochondrial dynamics controls T cell fate through metabolic programming. *Cell* **166**, 63–76 (2016).

42. Bolger, A.M., Lohse, M. & Usadel, B. Trimmomatic: a flexible trimmer for Illumina sequence data. *Bioinformatics* **30**, 2114–2120 (2014).
43. Li, H. & Durbin, R. Fast and accurate long-read alignment with Burrows–Wheeler transform. *Bioinformatics* **26**, 589–595 (2010).
44. McKenna, A. *et al.* The Genome Analysis Toolkit: a MapReduce framework for analyzing next-generation DNA sequencing data. *Genome Res.* **20**, 1297–1303 (2010).
45. Lek, M. *et al.* Analysis of protein-coding genetic variation in 60,706 humans. *Nature* **536**, 285–291 (2016).
46. Boeva, V. *et al.* Control-FREEC: a tool for assessing copy number and allelic content using next-generation sequencing data. *Bioinformatics* **28**, 423–425 (2012).
47. Carvalho, B.S. & Irizarry, R.A. A framework for oligonucleotide microarray preprocessing. *Bioinformatics* **26**, 2363–2367 (2010).
48. Luo, W., Friedman, M.S., Shedden, K., Hankenson, K.D. & Woolf, P.J. GAGE: generally applicable gene set enrichment for pathway analysis. *BMC Bioinformatics* **10**, 161 (2009).
49. Kamburov, A., Stelzl, U., Lehrach, H. & Herwig, R. The ConsensusPathDB interaction database: 2013 update. *Nucleic Acids Res.* **41**, D793–D800 (2013).
50. Brummer, T. *et al.* Phosphorylation-dependent binding of 14-3-3 terminates signalling by the Gab2 docking protein. *EMBO J.* **27**, 2305–2316 (2008).
51. Wilhelm, K. *et al.* Graft-versus-host disease enhanced by extracellular adenosine triphosphate activating P2X7R. *Nat. Med.* **16**, 1434–1438 (2010).
52. Schwab, L. *et al.* Neutrophil granulocytes recruited upon translocation of intestinal bacteria enhance GvHD via tissue damage. *Nat. Med.* **20**, 648–654 (2014).
53. Kaplan, D.H. *et al.* Target antigens determine graft-versus-host disease phenotype. *J. Immunol.* **173**, 5467–5475 (2004).

## Erratum: Sorafenib promotes graft-versus-leukemia activity in mice and humans through IL-15 production in FLT3-ITD-mutant leukemia cells

Nimitha R Mathew, Francis Baumgartner, Lukas Braun, David O'Sullivan, Simone Thomas, Miguel Waterhouse, Tony A Müller, Kathrin Hanke, Sanaz Taromi, Petya Apostolova, Anna L Illert, Wolfgang Melchinger, Sandra Duquesne, Annette Schmitt-Graeff, Lena Osswald, Kai-Li Yan, Arnim Weber, Sonia Tugues, Sabine Spath, Dietmar Pfeifer, Marie Follo, Rainer Claus, Michael Lübbert, Christoph Rummelt, Hartmut Bertz, Ralph Wäsch, Johanna Haag, Andrea Schmidts, Michael Schultheiss, Dominik Bettinger, Robert Thimme, Evelyn Ullrich, Yakup Tanriver, Giang Lam Vuong, Renate Arnold, Philipp Hemmati, Dominik Wolf, Markus Ditschkowski, Cordula Jilg, Konrad Wilhelm, Christian Leiber, Sabine Gerull, Jörg Halter, Claudia Lengerke, Thomas Pabst, Thomas Schroeder, Guido Kobbe, Wolf Rösler, Soroush Doostkam, Stephan Meckel, Kathleen Stabla, Stephan K Metzelder, Sebastian Halbach, Tilman Brummer, Zehan Hu, Joern Dengjel, Björn Hackanson, Christoph Schmid, Udo Holtick, Christof Scheid, Alexandros Spyridonidis, Friedrich Stölzel, Rainer Ordemann, Lutz P Müller, Flore Sicre-de-Fontbrune, Gabriele Ihorst, Jürgen Kuball, Jan E Ehlert, Daniel Feger, Eva-Maria Wagner, Jean-Yves Cahn, Jacqueline Schnell, Florian Kuchenbauer, Donald Bunjes, Ronjon Chakraverty, Simon Richardson, Saar Gill, Nicolaus Kröger, Francis Ayuk, Luca Vago, Fabio Ciceri, Antonia M Müller, Takeshi Kondo, Takanori Teshima, Susan Klaeger, Bernhard Kuster, Dennis (Dong Hwan) Kim, Daniel Weisdorf, Walter van der Velden, Daniela Dörfel, Wolfgang Bethge, Inken Hilgendorf, Andreas Hochhaus, Geoffroy Andrieux, Melanie Börries, Hauke Busch, John Magenau, Pavan Reddy, Myriam Labopin, Joseph H Antin, Andrea S Henden, Geoffrey R Hill, Glen A Kennedy, Merav Bar, Anita Sarma, Donal McLornan, Ghulam Mufti, Betul Oran, Katayoun Rezvani, Omid Shah, Robert S Negrin, Arnon Nagler, Marco Prinz, Andreas Burchert, Andreas Neubauer, Dietrich Beelen, Andreas Mackensen, Nikolas von Bubnoff, Wolfgang Herr, Burkhard Becher, Gerard Socié, Michael A Caligiuri, Eliana Ruggiero, Chiara Bonini, Georg Häcker, Justus Duyster, Jürgen Finke, Erika Pearce, Bruce R Blazar & Robert Zeiser

*Nat. Med.* 24, 282–291 (2018); published online 12 February 2018; corrected after print 6 March 2018

In the version of this article initially published, Omid Shah's name was misspelled as Omid Sha. The error has been corrected in the PDF and HTML versions of this article.

## Life Sciences Reporting Summary

Nature Research wishes to improve the reproducibility of the work that we publish. This form is intended for publication with all accepted life science papers and provides structure for consistency and transparency in reporting. Every life science submission will use this form; some list items might not apply to an individual manuscript, but all fields must be completed for clarity.

For further information on the points included in this form, see [Reporting Life Sciences Research](#). For further information on Nature Research policies, including our [data availability policy](#), see [Authors & Referees](#) and the [Editorial Policy Checklist](#).

### ► Experimental design

#### 1. Sample size

Describe how sample size was determined.

For the sample size in the murine GvL experiments, power analysis was performed. A sample size of at least  $n = 8$  per group was determined by 80% power to reach statistical significance of 0.05 to detect an effect size of at least 1.06. For the xenograft model,  $n=7$  per group was used because of the higher difference expected in this experimental setting. These long descriptions were included in the supplementary materials and methods section (section: statistical analysis) and not in the individual figure legends.

#### 2. Data exclusions

Describe any data exclusions.

All samples or mice were included in our analysis. This statement is included in the supplementary materials and methods (section: statistical analysis) part of the manuscript.

#### 3. Replication

Describe whether the experimental findings were reliably reproduced.

All the experimental findings were reliably reproduced.

#### 4. Randomization

Describe how samples/organisms/participants were allocated into experimental groups.

There was no randomization of mice or samples before analysis. Therefore, all samples or mice were included in our analysis. This statement is included in the supplementary materials and methods (section: statistical analysis) part of the manuscript.

#### 5. Blinding

Describe whether the investigators were blinded to group allocation during data collection and/or analysis.

The experiments were performed in a non-blinded fashion except for the GVHD severity scoring. To obtain unbiased data, the histopathology scoring of the GvHD severity was performed by a pathologist blinded to the genotype or treatment group. Only after finalization of the quantitative GvHD severity scores the samples were allocated to their genotypes/treatment group. This statement is included in the supplementary materials and methods (section: statistical analysis) part of the manuscript.

Note: all studies involving animals and/or human research participants must disclose whether blinding and randomization were used.

## 6. Statistical parameters

For all figures and tables that use statistical methods, confirm that the following items are present in relevant figure legends (or in the Methods section if additional space is needed).

n/a Confirmed

- The exact sample size ( $n$ ) for each experimental group/condition, given as a discrete number and unit of measurement (animals, litters, cultures, etc.)
- A description of how samples were collected, noting whether measurements were taken from distinct samples or whether the same sample was measured repeatedly
- A statement indicating how many times each experiment was replicated
- The statistical test(s) used and whether they are one- or two-sided (note: only common tests should be described solely by name; more complex techniques should be described in the Methods section)
- A description of any assumptions or corrections, such as an adjustment for multiple comparisons
- The test results (e.g.  $P$  values) given as exact values whenever possible and with confidence intervals noted
- A clear description of statistics including central tendency (e.g. median, mean) and variation (e.g. standard deviation, interquartile range)
- Clearly defined error bars

See the web collection on [statistics for biologists](#) for further resources and guidance.

## ► Software

Policy information about [availability of computer code](#)

### 7. Software

Describe the software used to analyze the data in this study.

The statistical analysis was performed using GraphPad Prism5 Version 5.03. The flow cytometry data was analyzed using Flow Jo software version 7.6.5 and version 10.2 (Tree Star, USA). The signals from western blots were quantified using LabImage 1D L340 version 4.1 (Intas Science Imaging GmbH, Germany) or ImageJ1.47i (NIH, USA) software. Bioluminescence imaging data were quantified with Living Image 3.2 software (Caliper Life Science, USA), further we used Genome Analysis Toolkit, Varscan2, Human reference genome hg19 using BWA aligner, Beacon Designer software (Premier Biosoft, UK), Patient data were analyzed using SAS 9.2 (SAS Institute Inc., Cary, NC, USA), western blots were quantified by LabImage 1D software or ImageJ software. MS dat were analyzed by MaxQuant software version 1.4.1.2 and version 1.5.3.30.

For manuscripts utilizing custom algorithms or software that are central to the paper but not yet described in the published literature, software must be made available to editors and reviewers upon request. We strongly encourage code deposition in a community repository (e.g. GitHub). *Nature Methods* [guidance for providing algorithms and software for publication](#) provides further information on this topic.

## ► Materials and reagents

Policy information about [availability of materials](#)

### 8. Materials availability

Indicate whether there are restrictions on availability of unique materials or if these materials are only available for distribution by a for-profit company.

There are no restrictions on the availability of materials used in this study.

### 9. Antibodies

Describe the antibodies used and how they were validated for use in the system under study (i.e. assay and species).

We provide a citation, catalog number and the clone number of all applied antibodies in Suppl. Table 12 and in the supplementary materials and methods (sections: 1) western blotting 2) Immunohistochemistry for IL-15 and phospho-IRF7 from Human BM biopsies and 3) In vivo depletion of IL-15) part of the manuscript. Suppl. Table 12: Antibodies for flow cytometry  
In the following we provide in the following order:

Antibody Clone	Catalogue number	Flouochrome	Vendor	Citation (Ref in Suppl.)
Anti-mouse CD3	17A2 100213	PB	Biolegend	6
Anti-mouse CD3	17A2 100233	BV510	Biolegend	7
Anti-mouse CD3ε	145-2C11 100309	PE-Cy5	Biolegend	8
Anti-mouse CD3	17A2 100215	Alexa flour 700	Biolegend	9
Anti-human CD3	SK7 344804	FITC	Biolegend	10
Anti-mouse CD4	RM4-5 100531	PB	Biolegend	11

## 10. Eukaryotic cell lines

a. State the source of each eukaryotic cell line used.

The following murine cell lines and cells were used: FLT3-ITD transfected Ba/F3 cells (Ba/F3-ITD), FLT3-ITD and luciferase transfected Ba/F3-ITD cells (Ba/F3-ITD-luc) provided by Dr. J. Duyster (Freiburg University Medical Centre). AML MLL-PTD FLT3-ITD leukemic cells were provided by Dr. B. R. Blazar (University of Minnesota). The murine cell lines, RMB1 and M1 were purchased from DSMZ, Germany. WEHI-3B cells were purchased from ATCC. The human cell lines, SKNO-156, KG-157, KG-1a58, ML-259, HL-6060, THP-161, KASUMI-162 and NB-463 were provided by Dr. M. Lübbert (Freiburg University Medical Centre). MOLM-13 cells were provided by Dr. T. Brummer (University of Freiburg). The human FLT3-ITD AML cell line MV4-1164 was provided by Dr. J. Finke (Freiburg University Medical Centre). All the cell lines which were used for in vivo experiments were authenticated at DSMZ or Multiplexion, Germany. The human cell lines, MOLM-13 cells and MV4-11 cells were authenticated by STR profiling. The murine cell lines were authenticated by COI species analysis to trace them back to their donor mouse strains.

b. Describe the method of cell line authentication used.

All the cell lines which were used for in vivo experiments were authenticated at DSMZ or Multiplexion, Germany. The human cell lines, MOLM-13 cells and MV4-11 cell were authenticated by STR profiling. The murine cell lines were authenticated by COI species analysis to trace them back to their donor mouse strains. This statement is included in the supplementary materials and methods (section: leukemia cell lines and cells) part of the manuscript .

c. Report whether the cell lines were tested for mycoplasma contamination.

All the cell lines have been repeatedly tested for Mycoplasma contamination and were found to be negative. This statement is included in the supplementary materials and methods (section: leukemia cell lines and cells) part of the manuscript.

d. If any of the cell lines used are listed in the database of commonly misidentified cell lines maintained by [ICLAC](#), provide a scientific rationale for their use.

None of the used cell lines are listed in the database of commonly misidentified cell lines.

## ► Animals and human research participants

Policy information about [studies involving animals](#); when reporting animal research, follow the [ARRIVE guidelines](#)

### 11. Description of research animals

Provide details on animals and/or animal-derived materials used in the study.

C57BL/6 (H-2Kb, Thy-1.2), BALB/c (H-2Kd, Thy-1.2), NSG mice and Rag2-/-Il2ry-/- mice were purchased either from Charles River Laboratory (Sulzfeld, Germany), Janvier Labs (France) or from the local stock of the animal facility at University of Freiburg. Il-15-/- mice were provided by Dr. Y. Tanriver (University of Freiburg). Il-15R $\alpha$ -/- mice were provided by Dr. B. Becher (University of Zurich). Mice were used between 6 and 12 weeks of age and only female or male donor/recipient pairs were used. Animal protocols (Protocol numbers: G13-116, G-15/018, G-16/018, G-17/093) were approved by the Regierungspräsidium Freiburg, Freiburg, Germany (Federal Ministry for Nature, Environment and Consumers` Protection).

## 12. Description of human research participants

Describe the covariate-relevant population characteristics of the human research participants.

The patients' median age was 50 (14-76) in the chemotherapy cohort, 50 (12-76) in the DLI alone cohort, 52 (20-76) in the DLI plus chemotherapy cohort, 53 (19-74) in the sorafenib alone cohort and 49 (18-68) in the sorafenib and DLI cohort.

The gender distribution was as follows:

chemotherapy cohort

female 49.5 (47)

male 50.5 (48)

DLI alone cohort

female 53.4 (63)

male 46.6 (55)

DLI plus chemotherapy cohort

female 51.6 (33)

male 48.4 (31)

sorafenib alone cohort

female 53.2 (41)

male 46.8 (36)

DLI plus sorafenib cohort

female 56.4 (31)

male 43.6 (24)

Additional characteristics, including AML characteristics, donor type, conditioning regimen, immunosuppressive regimen and remission status before transplant are detailed in Suppl. Table 1 for each individual patient. The data for each treatment group are summarized in Suppl. Tables 2-11.

## Flow Cytometry Reporting Summary

Form fields will expand as needed. Please do not leave fields blank.

### ▶ Data presentation

For all flow cytometry data, confirm that:

- 1. The axis labels state the marker and fluorochrome used (e.g. CD4-FITC).
- 2. The axis scales are clearly visible. Include numbers along axes only for bottom left plot of group (a 'group' is an analysis of identical markers).
- 3. All plots are contour plots with outliers or pseudocolor plots.
- 4. A numerical value for number of cells or percentage (with statistics) is provided.

### ▶ Methodological details

5. Describe the sample preparation.

For flow cytometry analysis from cell populations in splenocytes, spleens were isolated, homogenized and cells were filtered through a 70µm cell strainer and washed with cold 1X PBS. For flow cytometry analysis from cell populations in bone marrow, femur and tibia were isolated and sterilised with 70% ethanol. The bones were cut open and were flushed with cold 1X PBS using a syringe. The cells were filtered through a 70µm cell strainer and washed with cold 1X PBS. Before labelling the cells with antibodies for flow cytometry, the erythrocytes were eliminated from the samples by incubating with 3-5 ml erythrocyte lysis buffer for 4 min at RT. The reaction was stopped by adding 1X PBS and the cells were washed by centrifugation at 300xg for 8 min at 4°C. For flow cytometry, 1 x 10<sup>5</sup> - 1 x 10<sup>6</sup> cells were suspended in 100µl of cold 1XPBS in a round-bottom 96 well plate or a FACS tube.

For flow cytometry analysis from CD8+ Tc population of human subjects, human blood was withdrawn into a sterile EDTA coated S-Monovette (Sarstedt, Germany). The blood was mixed with two volumes of 1X PBS and overlaid onto one volume of Pancoll Human (PAN-Biotech, Germany). A gradient centrifugation was performed at 440xg for 30 minutes at room temperature to separate PBMC. The separated PBMC were collected from the interphase and washed with 1X PBS for flow cytometry staining.

6. Identify the instrument used for data collection.

We used three instruments:

- 1) CyAn ADP (Beckman Coulter) (Instance number: 1614193, serial number: 693)
- 2) BD LSRFortessa cell analyser (Model number: 647788E3, catalogue number: 647788)
- 3) BD LSRFortessa cell analyser (Model number: 649225B4, catalogue number: 649225)

7. Describe the software used to collect and analyze the flow cytometry data.

The flow cytometry data was collected by Summit v4.3. or BD FACSDIVA software. All flow cytometry data were analyzed by Flow Jo software version 7.6.5 and version 10.2 (Tree Star, USA)

8. Describe the abundance of the relevant cell populations within post-sort fractions.

The relevant cell populations are sorted using BD FACSARIA III cell sorter or using MACS cell sorting (Miltenyi Biotec). The cell purity was analyzed by

flow cytometry by comparing the cell populations before and after sorting. All the post-sort fractions were at least 90% pure.

9. Describe the gating strategy used.

The gating strategy of all relevant experiments is provided in the Supplementary Figure 14.

Tick this box to confirm that a figure exemplifying the gating strategy is provided in the Supplementary Information.